

# Luminescent First-Row Transition Metal Complexes

Christina Wegeberg and Oliver S. Wenger\*

Cite This: *JACS Au* 2021, 1, 1860–1876

Read Online

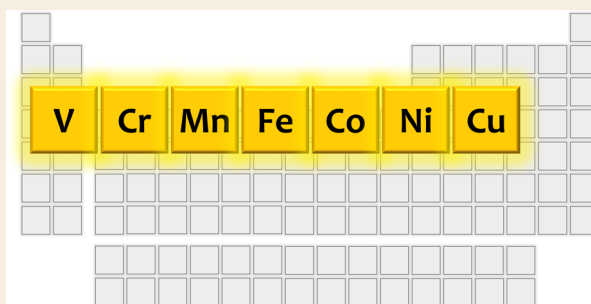
ACCESS |

Metrics & More

Article Recommendations

**ABSTRACT:** Precious and rare elements have traditionally dominated inorganic photophysics and photochemistry, but now we are witnessing a paradigm shift toward cheaper and more abundant metals. Even though emissive complexes based on selected first-row transition metals have long been known, recent conceptual breakthroughs revealed that a much broader range of elements in different oxidation states are useable for this purpose. Coordination compounds of V, Cr, Mn, Fe, Co, Ni, and Cu now show electronically excited states with unexpected reactivity and photoluminescence behavior. Aside from providing a compact survey of the recent conceptual key advances in this dynamic field, our Perspective identifies the main design strategies that enabled the discovery of fundamentally new types of 3d-metal-based luminophores and photosensitizers operating in solution at room temperature.

**KEYWORDS:** Photoluminescence, first-row transition metal complexes, coordination chemistry, metal-to-ligand charge transfer, ligand-to-metal charge transfer, Earth-abundant metals



## 1. INTRODUCTION

Many coordination compounds with platinum group metals have rich photophysical and electrochemical properties,<sup>1,2</sup> but their electronic structures are difficult to emulate with first-row transition metals. The key challenge is that a given coordination environment imposes a considerably weaker ligand field on a 3d-metal than on a 4d- or 5d-species, because the more contracted 3d-orbitals have weaker spatial overlaps with the relevant ligand orbitals than the 4d- or 5d-orbitals (Figure 1a).<sup>3</sup> Consequently, complexes with partially filled 3d-orbitals typically feature a multitude of metal-centered (MC) excited states, which are energetically close to each other and to the electronic ground state. This scenario is problematic, because it can allow for a cascade of nonradiative relaxation processes from one MC state to the other and finally back to the ground state (Figure 1b).<sup>4</sup> Moreover, in some of the MC states, the metal–ligand bonding situation is very different from the ground state, for example, when d-electrons are promoted from nonbonding to antibonding orbitals. The respective excited states are then said to be “distorted”, and this is captured by the displacement of potential wells along a certain nuclear coordinate (Figure 1b/c), for instance, the metal–ligand bond distance.<sup>5</sup> From the resulting overall picture, it is quite obvious that the barriers for crossing from one potential well into the next lower one can be undesirably low, causing rapid nonradiative relaxation.

The stronger ligand fields of 4d- and 5d-metal complexes typically do not only lead to greater energy gaps between the individual MC states, but also to a sizable energy gap between

the lowest MC state and the electronic ground state (Figure 1c). In such cases, that lowest MC state can become luminescent and photochemically active,<sup>5</sup> because nonradiative relaxation becomes less efficient when the excitation energy has to be dissipated by an increasing number of vibrational quanta.<sup>6</sup> Energetically high lying MC states furthermore open the possibility for the installment of fundamentally different excited states at lower energies (while maintaining a sufficiently large gap to the ground state), for instance states, in which electron density is shifted from the metal to the ligands or vice versa. Since the lowest excited state commonly governs the photophysical and photochemical properties, that state is usually the most important one, and the aforementioned metal-to-ligand charge transfer (MLCT) and ligand-to-metal charge transfer (LMCT) are very attractive for many applications. The redox properties in these charge-transfer states are drastically altered with respect to the ground state, enabling them to engage in photoredox chemistry with organic substrates<sup>7,8</sup> or to act as dyes in inorganic semiconductor solar cells.<sup>9</sup> Ligand-to-ligand charge transfer (LLCT), in which electron density is shifted from one coordinated ligand to another, can be similarly useful.<sup>10</sup> This is fundamentally

Received: August 13, 2021

Published: September 24, 2021



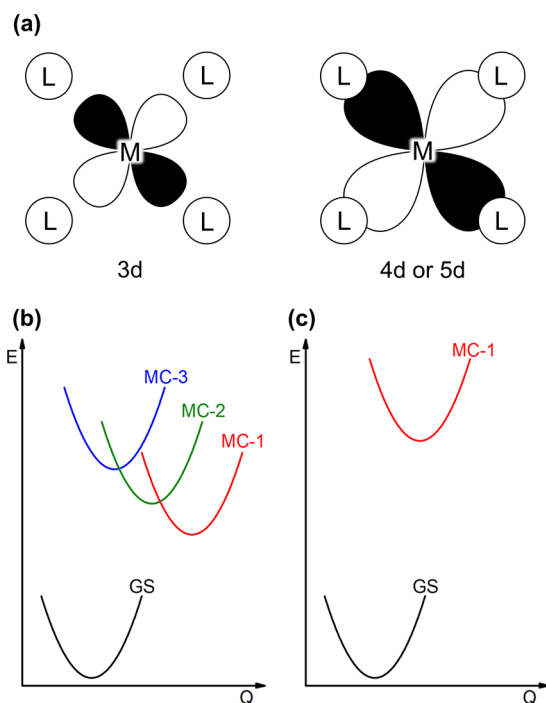


**Figure 1.** (a) Illustration of the overlap between metal d-orbitals and ligand orbitals. (b) Exemplary single configurational coordinate diagram for a 3d-metal complex (c) Exemplary single configurational coordinate diagram for a 4d- or 5d-metal complex. Q is a nuclear coordinate.

different from so-called intraligand (IL) excitations, in which the electron density redistribution typically occurs within the  $\pi$ -conjugation system of a given (individual) ligand.

Contrary to typical organic compounds, many metal complexes facilitate rapid intersystem crossing from initially excited singlet to lower-lying triplet excited states by virtue of strong spin–orbit coupling.<sup>11</sup> This is important because triplet states give access to photochemical reactivities that are unattainable from singlets, they can have improved kinetic reactivity due to longer lifetimes,<sup>12</sup> and photoinduced electron transfer from triplet states can produce primary photoproducts that undergo less (undesired) charge recombination, leading to inherently greater quantum efficiencies of photoredox reactions.<sup>12,13</sup> Numerous applications underscore the important role played by (so far mostly precious) metal-based compounds, including luminophores in organic light emitting diodes (OLEDs)<sup>14</sup> and light-emitting electrochemical cells (LEECs),<sup>15,16</sup> photocatalysts in synthetic photochemistry and artificial photosynthesis,<sup>17,18</sup> light-harvesters in dye-sensitized solar cells,<sup>19</sup> and sensitizers in photochemical upconversion or photodynamic therapy.<sup>20,21</sup> Thus, there are many good reasons to search for photoactive complexes based on cheap and abundant metals.<sup>22–24</sup>

Copper(I) emerged as an attractive candidate nearly 40 years ago,<sup>25</sup> and furthermore, some chromium(III) complexes had long been known to emit in solution at room temperature (Figure 2).<sup>26</sup> With both metal ions, key conceptual progress has been made recently, and complexes with exceptional luminescence quantum yields and excited-state lifetimes were reported.<sup>27</sup> For other elements such as cobalt and nickel, there had been a few selected reports on emission from molecular complexes in the older literature,<sup>28</sup> but just recently several studies revived interest in these two elements that were long

Sc	Ti	V	Cr	Mn	Fe	Co	Ni	Cu	Zn
d <sup>0</sup>	d <sup>0</sup>	d <sup>2</sup>	d <sup>3</sup>	d <sup>3</sup>	d <sup>5</sup>	d <sup>6</sup>	d <sup>8</sup>	d <sup>10</sup>	
+III	+IV	+III	+III	+IV	+III	+III	+II	+I	
			d <sup>6</sup>	d <sup>6</sup>					
			0	+I					

**Figure 2.** Red: Elements for which luminescent complexes have long been known but important conceptual progress has been made recently. Yellow: A few selected luminescent complexes were known for these elements, and a few more examples have been added recently. Green: New elements on the landscape of emissive molecular complexes in solution at room temperature. Gray: Many luminescent Zn<sup>II</sup> complexes are known, but they typically feature ligand-centered emission. White: Elements for which room temperature emission in solution still remains a challenge and no recent reports have appeared. Spin states and appertaining oxidation states of so far known examples of luminescent molecular complexes in solution at room temperature are listed below the individual elements.

neglected in molecular photophysics and photochemistry. As the most abundant transition metal element in Earth's crust, iron continuously attracts much attention, but two recent landmark studies<sup>29,30</sup> lead to unexpected insight that could revolutionize the field.<sup>31</sup> Manganese and vanadium represent two comparatively abundant d-metal elements that only just appeared on the landscape of molecular complexes showing luminescence in solution at room temperature.<sup>32–34</sup>

The focus of our Perspective is on the recent conceptual key discoveries in the field of molecular complexes with first-row transition metals that luminesce in solution at room temperature. When a compound emits under these conditions, this typically implies excited-state lifetimes that are sufficiently long for diffusion-controlled bimolecular reactions; hence, these compounds can in principle become suitable for photochemical applications that go far beyond simple lighting, and we then call those complexes “photoactive”.<sup>23</sup> Of particular interest here is the direct involvement of the metal in shaping the photophysical and photochemical properties, whereas complexes in which IL excitations play a dominant role (such as, for example, in many zinc(II) compounds)<sup>35</sup> are not considered. Our Perspective is structured into four core sections for the four main types of photoactive excited states (LLCT, MLCT, LMCT, and MC) that are relevant for the various 3d<sup>n</sup>-electron configurations ( $n = 2–10$ ). Based on the conceptual insights gained from this survey, we then give a brief outlook into the possible future of luminescent base metal complexes.

## 2. LLCT EMITTERS: 3d<sup>10</sup> (Cu<sup>I</sup>) COMPLEXES

In the 3d<sup>10</sup> electron configuration, there are no energetically low-lying MC states, and therefore, emissive MLCT and LLCT excited states can be installed comparatively easily. Homoleptic bis( $\alpha$ -diimine)copper(I) as well as heteroleptic variants combining  $\alpha$ -diimine with diphosphine ligands have attracted much attention in the past,<sup>19,36</sup> but recent work demonstrated that such four-coordinate tetrahedral Cu<sup>I</sup> MLCT luminophores are outperformed by two-coordinate linear Cu<sup>I</sup> LLCT emitters.<sup>37</sup> The combination of unconventional N-heterocyclic carbenes with N-bound amide ligands leads to charge-neutral Cu<sup>I</sup> compounds featuring luminescence quantum yields approaching 100% in the solid state and in solution at room temperature (Figure 3a).<sup>38,39</sup> The (anionic) amide ligands are

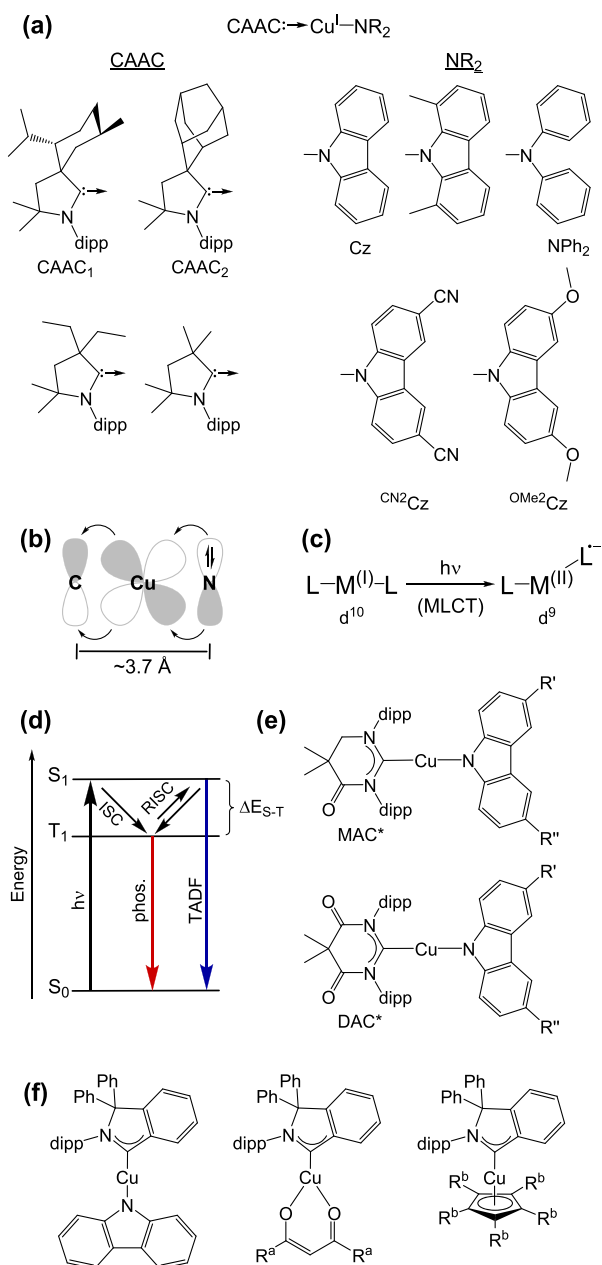


**Figure 3.** (a) Linear molecular structure of two-coordinate CAAC-Cu<sup>I</sup>-amido complexes (at the top) and structures of exemplary CAAC and amido ligands.<sup>38</sup> (b) Key frontier orbitals in CAAC-Cu<sup>I</sup>-amido complexes and direction of charge transfer upon LLCT excitation.<sup>38</sup> (c) Renner-Teller distortion upon MLCT excitation of linear d<sup>10</sup> complexes.<sup>41</sup> (d) Energy-level diagram illustrating emission processes of CAAC-Cu<sup>I</sup>-amido complexes.<sup>39</sup> (e) Molecular structures of linear Cu<sup>I</sup> complexes based on cyclic mono- or diamidocarbene ligands.<sup>39</sup> (f) Molecular structures of some exemplary CAAC-Cu<sup>I</sup> complexes.<sup>45</sup> R<sup>c</sup> = H, CN, R<sup>b</sup> = H, CN, R<sup>a</sup> = CH<sub>3</sub>, Ph, R<sup>b</sup> = H, CH<sub>3</sub>, <sup>CN</sup>Cz, when R<sup>c</sup> = CN and R<sup>b</sup> = H.

strong  $\pi$ -electron donors, whereas cyclic (alkyl)(amino)-carbene (CAAC) ligands (or related unconventional *N*-heterocyclic carbenes) act as  $\pi$ -acceptors, leading to luminescence from an LLCT excited state. This is a key conceptual difference to traditional four-coordinate Cu<sup>I</sup> complexes, which have photoactive MLCT states that undergo Jahn-Teller distortion with a consequent increase of nonradiative decay rates.<sup>40</sup> In the new linear compounds, the metal

remains of key importance, as it mediates significant electronic coupling between the donor and acceptor ligands through its d-orbitals (Figure 3b) and furthermore facilitates intersystem crossing (ISC) between singlet and triplet states. As long as both ligands are coplanar (such as the case in the S<sub>0</sub> and T<sub>1</sub> states of suitably designed complexes), the LLCT is strongly allowed both in absorption and emission,<sup>38</sup> meaning that extinction coefficients are sizable (4000–6000 M<sup>-1</sup> cm<sup>-1</sup>) despite considerable donor-acceptor distances (ca. 3.7 Å) and radiative decay rates (*k<sub>r</sub>*) are comparatively high (ca. 10<sup>5</sup>–10<sup>6</sup> s<sup>-1</sup>). Nonradiative relaxation is decelerated by steric encumbrance on the carbene ligands (Figure 3a), in part because this prevents undesired bending (Renner-Teller) distortions (Figure 3c).<sup>41</sup> The limited metal character associated with the photoactive excited state(s) is beneficial for minimization of the Renner-Teller distortion.<sup>39</sup>

Since the HOMO and the LUMO are spatially well separated, the singlet-triplet energy gap ( $\Delta E_{S-T}$ ) of the emissive LLCT state can become small enough such that S<sub>1</sub> can be repopulated from T<sub>1</sub> via reverse intersystem crossing (RISC), causing a situation reminiscent of thermally activated delayed fluorescence (TADF), though neither the singlet nor the triplet is spin-pure in these Cu<sup>I</sup> complexes (Figure 3d).<sup>38,39</sup> Thus,  $\Delta E_{S-T}$  remains small while *k<sub>r</sub>* of the luminescence process is comparatively large, two properties which are usually considered mutually exclusive but highly desirable for TADF emitters. Consequently, light-emitting diodes with outstanding quantum efficiencies become possible.<sup>38,42</sup>

Variations of the donor and acceptor ligands of the linear Cu<sup>I</sup> complexes permit emission color tuning over the entire visible spectral range (Table 1), for example, when combining cyclic monoamidocarbene (MAC\*) or cyclic diamidocarbene (DAC\*) ligands with carbazoles (Figure 3e).<sup>39</sup> The carbonyl groups of these carbenes enhance their  $\pi$ -acceptor properties, and their bulky 2,6-diisopropylphenyl (dipp) substituents suppress the formation of exciplexes with solvent molecules; one of the most common nonradiative deactivation pathways for traditional Cu<sup>I</sup> complexes.<sup>40,43,44</sup> Cyclic (amino)(aryl)-carbenes (CAACs) have a more extended  $\pi$ -system (Figure 3f) and are more electrophilic than their alkyl counterparts (CAACs), leading to a substantial red-shift of the lowest-energy UV-vis absorption bands and providing access to deep red and near-infrared (NIR) luminophores.<sup>45</sup> High radiative rate constants and small singlet-triplet energy gaps remain unusually low triplet energies and promising TADF properties.

Traditional four-coordinate Cu<sup>I</sup> complexes<sup>25,53</sup> as well as polynuclear Cu<sup>I</sup> compounds<sup>54–56</sup> continue to receive significant attention,<sup>57–62</sup> yet much of this work has been reviewed and will not be considered further here.<sup>15,19,36,63</sup>

### 3. MLCT EMITTERS: 3d<sup>6</sup> (Mn<sup>I</sup> and Cr<sup>0</sup>) COMPLEXES AND A 3d<sup>8</sup> (Ni<sup>II</sup>) COMPOUND

Metal complexes with the 4d<sup>6</sup> and 5d<sup>6</sup> valence electron configurations, in particular with Ru<sup>II</sup>, Re<sup>I</sup>, Os<sup>II</sup>, and Ir<sup>III</sup>, are among the most widely employed MLCT emitters.<sup>1,2,64</sup> The idea of obtaining analogous <sup>3</sup>MLCT luminescence from 3d<sup>6</sup> complexes is attractive, among other things because the above-mentioned metals are all very precious and rare. Most efforts until now have focused on iron, but no Fe<sup>II</sup> complexes emitting from an MLCT excited state under steady-state irradiation at room temperature have been reported to date.<sup>65</sup> The key problem is that the more contracted 3d-orbitals of Fe<sup>II</sup>

**Table 1. Complexes Emitting from Charge-Transfer Excited States and Some of Their Key Photophysical Properties in Deaerated Solution at Room Temperature**

compd	electron configuration	solvent	$\lambda_{em}$ [nm]	$\tau_0$	$\phi$ [%]	type of emission	ref
[Cu(MAC*)( <sup>CN2</sup> Cz)]	d <sup>10</sup>	2-MeTHF	448	2.3 $\mu$ s	24	LLCT	39
[Cu(MAC*)( <sup>CN</sup> Cz)]	d <sup>10</sup>	2-MeTHF	492	1.2 $\mu$ s	~100	LLCT	39
[Cu(MAC*)(Cz)]	d <sup>10</sup>	2-MeTHF	542	1.1 $\mu$ s	55	LLCT	39
[Cu(DAC*)( <sup>CN</sup> Cz)]	d <sup>10</sup>	2-MeTHF	666	52 ns	2	LLCT	39
[Cu(CAAC <sub>1</sub> )(Cz)]	d <sup>10</sup>	2-MeTHF	492	2.5 $\mu$ s	~100	LLCT	38
[Cu(CAAC <sub>2</sub> )(Cz)]	d <sup>10</sup>	2-MeTHF	510	2.3 $\mu$ s	68	LLCT	38
[Cu(CAAC <sub>1</sub> )( <sup>OMe2</sup> Cz)]	d <sup>10</sup>	2-MeTHF	558	0.28 $\mu$ s	25	LLCT	38
[Cu(CAAC <sub>1</sub> )(NPh <sub>2</sub> )]	d <sup>10</sup>	2-MeTHF	580	0.87 $\mu$ s	16	LLCT	38
[Cr(L <sup>tBu</sup> ) <sub>3</sub> ]	d <sup>6</sup>	THF	630	2.2 ns	0.001	MLCT	46
[Cr(L <sup>Pyr</sup> ) <sub>3</sub> ]	d <sup>6</sup>	cyclooctane	682	6.10 ns <sup>a</sup>	0.09	MLCT	47
[Mn(L <sup>bi</sup> ) <sub>3</sub> ] <sup>+</sup>	d <sup>6</sup>	CH <sub>3</sub> CN	485	0.74 ns <sup>b</sup>	0.05	MLCT	32
[Mn(L <sup>tri</sup> ) <sub>2</sub> ] <sup>+</sup>	d <sup>6</sup>	CH <sub>3</sub> CN	525	1.73 ns <sup>c</sup>	0.03	MLCT	32
[Ni(BuImp)(CH <sub>3</sub> CN)](PF <sub>6</sub> )	d <sup>8</sup>	solid state	534 <sup>d</sup>				48
[Ni(dpb)(Cz)]	d <sup>8</sup>	solid state	600 <sup>d</sup>	0.11 $\mu$ s <sup>d,e</sup>		IL/MLCT	49
[Cp* <sub>2</sub> ScCl]	d <sup>0</sup>	isooctane/methylcyclohexane (1:1)	520	2.0 $\mu$ s	0.01	LMCT	50
[Fe(bt <sub>z</sub> ) <sub>3</sub> ] <sup>3+</sup>	d <sup>5</sup>	CH <sub>3</sub> CN	600	0.1 ns	0.03	LMCT	29
[Fe(PhB(MeIm) <sub>3</sub> ) <sub>2</sub> ] <sup>+</sup>	d <sup>5</sup>	CH <sub>3</sub> CN	655	2.0 ns	2.1	LMCT	30
[Fe(ImP) <sub>2</sub> ] <sup>+</sup>	d <sup>5</sup>	CH <sub>3</sub> CN	450	4.2 ns <sup>f</sup>		MLCT	51
			675	0.22 ns	<1	LMCT	
[Co(dgpy) <sub>2</sub> ] <sup>3+</sup>	d <sup>6</sup>	CH <sub>3</sub> CN	440	5.07 ns	0.7	LMCT	52
[Co(dgpz) <sub>2</sub> ] <sup>3+</sup>	d <sup>6</sup>	CH <sub>3</sub> CN	412	6.55 ns <sup>g</sup>	0.4	LMCT	52

<sup>a</sup>Weighted average from biexponential decay fit (4.05 ns (48%), 8.00 ns (52%)). <sup>b</sup>Weighted average from a triexponential decay fit (0.374 ns (79.2%), 1.84 ns (19.3%), 5.85 ns (1.5%)). <sup>c</sup>Weighted average from a triexponential decay fit (0.635 ns (56.4%), 2.07 ns (33.6%), 6.74 ns (10.0%)). <sup>d</sup>Data obtained in the solid state. <sup>e</sup>Measured at 77 K. The emission maximum at 77 K is at 468 nm. <sup>f</sup>Average value, see original reference for details. <sup>g</sup>Weighted average from a biexponential decay fit (3.21 ns (39%), 8.69 ns (61%)).

experience a substantially weaker ligand field than the 4d-orbitals of Ru<sup>II</sup> (Figure 1a),<sup>3</sup> and in classical octahedral polypyridine complexes the metal-centered <sup>3</sup>T<sub>1g</sub> and <sup>5</sup>T<sub>2g</sub> excited states (Figure 4a) are energetically below the lowest MLCT state. Consequently, relaxation from the MLCT to these MC states is typically ultrafast (Figure 4b).<sup>66,67</sup> The MC states can indeed be exploited for photoredox reactions though they are nonemissive.<sup>68–71</sup> Recently, there has been important progress in elongating the lifetimes of dark MLCT states, as well as in understanding their population and deactivation pathways.<sup>72–76</sup> Much of this work has been reviewed,<sup>65,77–79</sup> and since these compounds are nonluminescent, they are not considered further here.

Following earlier work on W<sup>0</sup> arylisocyanides,<sup>81,82</sup> we found that chelating diisocyanide ligands give access to luminescent Mo<sup>0</sup> complexes.<sup>83–85</sup> This chemistry was further extendable to the first row of transition metals and resulted in a Cr<sup>0</sup> complex (L<sup>tBu</sup> ligand in Figure 4c, complex structure in Figure 4d) that emitted from a <sup>3</sup>MLCT state in solution at room temperature.<sup>46</sup> The emission quantum yield of [Cr(L<sup>tBu</sup>)<sub>3</sub>] is very low (ca. 10<sup>-5</sup>), but the MLCT lifetime of 2.2 ns in deaerated THF at 20 °C is remarkable (Table 1). The sterically demanding *tert*-butyl substituents in *ortho*-position to the isocyanide groups protect the metal center from the chemical environment and rigidify the overall complex. Such shielding and rigidification strategies are generally quite successful for improvement of chemical robustness and for the deceleration of nonradiative excited-state relaxation processes in photoactive metal complexes made from Earth-abundant metals.<sup>84,86,87</sup> Early studies reported on peculiar dual MLCT emission from several [Cr( $\alpha$ -diimine)(CO)<sub>4</sub>] complexes in benzene at room temperature.<sup>88,89</sup> It is not a priori obvious why two MLCT states, which are energetically relatively close

and distorted to different extents relative to each other, can both be emissive.<sup>90</sup> Furthermore, photoinduced CO-dissociation can be an important excited-state deactivation pathway in this compound class.<sup>91</sup> Be that as it may, the [Cr(L<sup>tBu</sup>)<sub>3</sub>] complex is a comparatively clear-cut 3d<sup>6</sup> MLCT emitter under continuous-wave irradiation at room temperature.

Attachment of pyrene moieties in the ligand backbone of the diisocyanide ligands in [Cr(L<sup>tBu</sup>)<sub>3</sub>] afforded the complex [Cr(L<sup>Pyr</sup>)<sub>3</sub>] (L<sup>Pyr</sup> ligand in Figure 4c, complex structure in 4d).<sup>47</sup> [Cr(L<sup>Pyr</sup>)<sub>3</sub>] showed an MLCT lifetime of 6.10 ns and an accompanying luminescence quantum yield of 0.09% in deaerated cyclooctane at 20 °C. The largely improved photophysical properties of [Cr(L<sup>Pyr</sup>)<sub>3</sub>] relative to those of [Cr(L<sup>tBu</sup>)<sub>3</sub>] are due to the delocalization effect.<sup>92–94</sup> The delocalization effect is a well-known strategy to improve photophysical properties of ruthenium(II) polypyridines, and [Cr(L<sup>Pyr</sup>)<sub>3</sub>] is the first 3d<sup>6</sup> emitter to benefit from this concept. Both the luminescence quantum yield and the MLCT lifetime of [Cr(L<sup>Pyr</sup>)<sub>3</sub>] showed an unusual bell-shaped solvent dependency, indicative of two counteracting effects controlling the MLCT deactivation giving rise to optimal emissive conditions in cyclooctane. The two effects were identified as predominantly deactivation either through an energetically nearby lying MC excited state in the most apolar solvents such as *n*-hexane or alternatively via direct nonradiative relaxation to the ground state in accordance with the energy gap law in more polar solvents such as 1,4-dioxane. A tetracarbonyl complex of Cr<sup>0</sup> with a bidentate pyridyl-mesoionic carbonyl ligand was recently reported to show near-infrared-II emission, albeit exclusively in the solid state.<sup>95</sup>

Recently, chelating isocyanide ligands enabled the synthesis and characterization of the first luminescent Mn<sup>I</sup> complexes.<sup>32</sup> Isoelectronic with Fe<sup>II</sup> and Cr<sup>0</sup>, they are 3d<sup>6</sup> MLCT emitters,

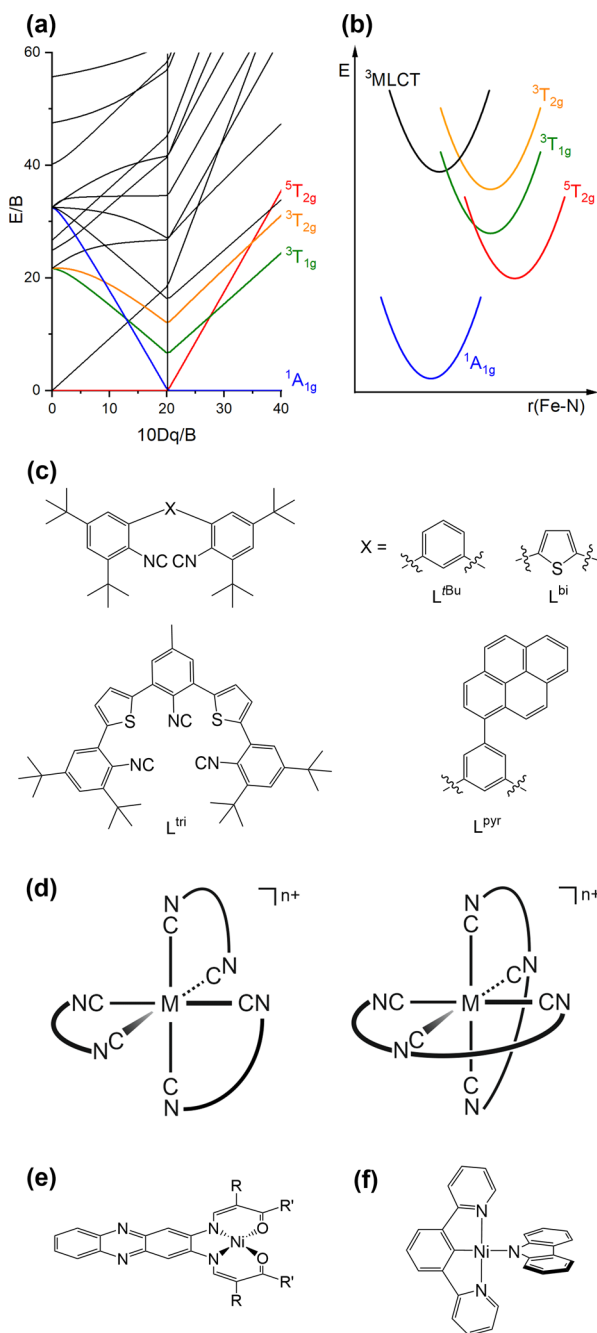


**Figure 4.** (a) Tanabe–Sugano diagram for the  $d^6$ -electron configuration in an octahedral ligand field. (b) Single configurational coordinate diagram involving some key electronic states in  $[\text{Fe}(\text{bpy})_3]^{2+}$ .<sup>66</sup> (c) Molecular structures of the isocyanide ligands  $L^{\text{fbu}}$ ,  $L^{\text{bi}}$ ,  $L^{\text{pyr}}$ , and  $L^{\text{tri}}$ . (d) Generic structures of homoleptic tris-(diisocyanide) and bis(triisocyanide) complexes.  $M = \text{Cr}^0$ ,  $n = 0$ ;  $\text{Mn}^1$ ,  $n = 1$ .<sup>32,46,47</sup> (e) Molecular structures of  $\text{Ni}^{\text{II}}$  complexes showing luminescence that strongly resembles ligand fluorescence ( $R = \text{COOEt}$ ,  $\text{COOMe}$ ;  $R' = \text{Me}$ ,  $\text{CF}_3$ ).<sup>80</sup> (f) Molecular structure of  $[\text{Ni}^{\text{II}}(\text{dpb})(\text{Cz})]$ .<sup>49</sup>

but the higher oxidation state with respect to  $\text{Cr}^0$  makes the  $\text{Mn}^1$  complexes more air-stable. The  $[\text{Mn}(\text{L}^{\text{bi}})_3]^+$  and  $[\text{Mn}(\text{L}^{\text{tri}})_2]^+$  complexes ( $L^{\text{bi}}$  and  $L^{\text{tri}}$  ligands in Figure 4c, complex structures in 4d) can be considered first-row analogues of the well-known  $[\text{Ru}(\text{bpy})_3]^{2+}$  and  $[\text{Ru}(\text{tpy})_2]^{2+}$  compounds, and they luminesce with quantum yields of 0.03–0.05% in acetonitrile at room temperature (Table 1). The strong ligand

field created by the  $\pi$ -acceptor isocyanide ligands shifts the detrimental  $^3\text{T}_{1g}$  and  $^5\text{T}_{2g}$  MC states (Figure 4a) to sufficiently high energies, such that blue MLCT emission can become competitive with nonradiative relaxation, though the comparatively low quantum yields indicate that dissipation of excitation energy by molecular vibrations remains the major relaxation pathway in this compound class, at least until now. The luminescence behavior of these tris(diisocyanide) and bis(triisocyanide) manganese(I) compounds stands in contrast to long-known  $\text{Mn}^1$  tricarbonyl diimines, which undergo efficient CO ligand release (due to the rapid population of the above-mentioned dissociative MC states), but no emission is accompanied by this process.<sup>4,96–98</sup> The MLCT lifetimes of  $[\text{Mn}(\text{L}^{\text{bi}})_3]^+$  and  $[\text{Mn}(\text{L}^{\text{tri}})_2]^+$  are on the order of 1–2 ns in  $\text{CH}_3\text{CN}$  at 20 °C, and this is long enough for bimolecular electron and (triplet–triplet) energy transfer reactions.<sup>32</sup> Thus, the manganese(I) isocyanide compounds exhibit the same type of photoreactivity as  $\text{Ru}^{\text{II}}$  polypyridines and cyclometalated  $\text{Ir}^{\text{III}}$  complexes. Though manganese is not as abundant as iron, its natural abundance in Earth's crust exceeds that of copper by a factor 18,<sup>99</sup> which seems noteworthy given the long-standing interest of the photophysics and photochemistry community in copper.

The photophysics and the photochemistry of molecular nickel(II) complexes recently gained considerable attention in the context of light-driven (or at least light-initiated) cross coupling catalysis,<sup>100–104</sup> though this typically involves non-emissive  $\text{Ni}^{\text{II}}$  compounds with energetically low-lying MC states that deactivate nonradiatively.<sup>105</sup> A recent study reported on unexpectedly intense photoluminescence from square-planar  $\text{Ni}^{\text{II}}$  complexes, where it seems that the emission is essentially due to a fluorescent ligand (Figure 4e).<sup>80</sup> Another very recent study had a clear focus on installing emissive charge-transfer states in  $\text{Ni}^{\text{II}}$  complexes and succeeded in identifying some key design principles for obtaining square-planar complexes that luminesce in the solid state at 298 K or in frozen glasses at 77 K.<sup>49</sup> The carbazolylnickel(II) complex in Figure 4f has a lowest-lying UV–vis absorption band attributable to a mixed IL (localized on the cyclometalating terdentate ligand) and MLCT excitation according to TD-DFT calculations. Weak luminescence at room temperature is observed, and at 77 K its lifetime is 0.11  $\mu\text{s}$ , suggesting an emissive triplet state. In the 77 K emission spectrum vibrational progressions in a skeletal vibration mode of the ligand framework (ca. 1400  $\text{cm}^{-1}$ ) point to a significant IL contribution. Nevertheless, it seems clear that the use of strong-field terdentate ligands is a promising route toward  $\text{Ni}^{\text{II}}$  complexes exhibiting MLCT luminescence.<sup>48,49</sup> So far, this has only been achievable with tetrahedral  $\text{Ni}^0$  complexes,<sup>106,107</sup> which exhibit comparable photophysical properties to four-coordinate  $\text{Cu}^1$  diimine complexes; however, tetrahedral  $\text{Ni}^0$  compounds tend to be very air-sensitive. Other new developments in  $\text{Ni}^{\text{II}}$  photochemistry involve the use of macrocyclic ligands, but no emission has been reported so far.<sup>108,109</sup>

#### 4. LMCT EMITTERS: $3d^0$ ( $\text{Sc}^{\text{III}}$ ), $3d^3$ ( $\text{Mn}^{\text{IV}}$ ), $3d^5$ ( $\text{Fe}^{\text{III}}$ ), AND $3d^6$ ( $\text{Co}^{\text{III}}$ ) COMPLEXES

Energetically low-lying LMCT states call for electron-rich ligands and electron-deficient metals. The most promising valence electron configuration for achieving long-lived LMCT states is  $d^0$ , because in this specific case there are no MC states through which the LMCT excited state can deactivate nonradiatively. Consequently, group 3 metals in the +III

oxidation state and group 4 metals in the +IV oxidation state are very promising candidates. Early on,  $[\text{Cp}^*_2\text{ScCl}]$  was found to emit in fluid solution at room temperature with a luminescence lifetime of 2.0  $\mu\text{s}$  and the emissive excited state was assigned as LMCT from the  $p\text{-Cl}$  nonbonding lone pair to the  $\text{Sc}^{3+}$  ion.<sup>50,110</sup> Many  $\text{Ti}^{\text{IV}}$  based metallocenes with the general formula  $\text{Cp}_2\text{TiX}_2$  also exhibit LMCT luminescence,<sup>111</sup> albeit typically only in the solid state at 77 K.<sup>112</sup> More recently, this compound class has become of interest for photoredox catalysis.<sup>113,114</sup> A  $\text{Ti}^{\text{IV}}$  carbene complex seemed to be nonemissive in solution at room temperatures while its  $\text{Zr}^{\text{IV}}$  and  $\text{Hf}^{\text{IV}}$  analogues emitted under these conditions.<sup>115</sup> Recent work on related work focused much on  $\text{Zr}^{\text{IV}}$  (and comparatively little on  $\text{Ti}^{\text{IV}}$ ), suggesting that room temperature emission is much more tricky to obtain for  $\text{Ti}^{\text{IV}}$  than for  $\text{Zr}^{\text{IV}}$ .<sup>87,116–118</sup>

The electron-donating tris(carbene)borate ligand  $\text{PhB}(\text{MeIm})_3$  stabilizes manganese in its +IV oxidation state,<sup>119</sup> and the homoleptic  $[\text{Mn}(\text{PhB}(\text{MeIm})_3)_2]^{2+}$  complex (Figure 5a,  $\text{M} = \text{Mn}^{\text{IV}}$ ,  $n = 2$ ) shows ruby-like red emission in the solid state at room temperature, similar to many isoelectronic  $\text{Cr}^{\text{III}}$  compounds. Unexpectedly, this compound furthermore shows green luminescence from an LMCT excited state (up to room temperature), even though several MC states of the  $d^3$  valence electron configuration are energetically lower. The green emission spectrum mirrors a corresponding LMCT absorption band with a high oscillator strength, indicative of a spin-allowed transition, which implies a high radiative decay rate constant that could be crucially important to make luminescence competitive with nonradiative relaxation. An emission lifetime of 50 ns at 85 K (where nonradiative relaxation should be largely suppressed) is compatible with this interpretation, and the vibrational fine structure in the emission spectrum (featuring progressions in the typical range of ligand breathing modes) further supports the LMCT assignment. This  $\text{Mn}^{\text{IV}}$  study was the first in a series of recent reports on unexpected LMCT emissions from 3d-metal complexes, in particular among the  $\text{Fe}^{\text{III}}$  compounds considered in the following.

*N*-Heterocyclic carbene (NHC) ligands caught the attention of the iron photophysics research community some time ago,<sup>77,78,120,121</sup> yet it was mostly the recent use of a mesoionic carbene (MIC) ligand (Figure 5b) that led to a conceptual breakthrough. While NHCs are merely strong  $\sigma$ -donors, MICs combine good  $\sigma$ -donor with strong  $\pi$ -acceptor properties, causing very strong ligand fields in which nonradiatively deactivating MC states are energetically destabilized and emissive charge-transfer excited states can instead become accessible.<sup>65</sup> The original aim with the btz ligand was likely to obtain an  $\text{Fe}^{\text{II}}$  compound with a long-lived MLCT state,<sup>122</sup> but the resulting homoleptic complex underwent facile oxidation to  $\text{Fe}^{\text{III}}$  (Figure 5b). Strikingly, the resulting  $[\text{Fe}(\text{btz})_3]^{3+}$  complex turned out to be photoluminescent,<sup>29</sup> which was not to be expected for a low-spin  $d^5$  complex. Given the presence of energetically low-lying MC states in this valence electron configuration, the observation of LMCT emission at room temperature is very surprising at first glance but can be rationalized on the basis of detailed spectroscopic and computational studies: First of all, the LMCT emission is spin-allowed and therefore has a high radiative rate constant. Second, the small Stokes shift between LMCT absorption and emission bands (0.15 eV) indicates that the LMCT state is only weakly distorted with respect to the ground state (Figure

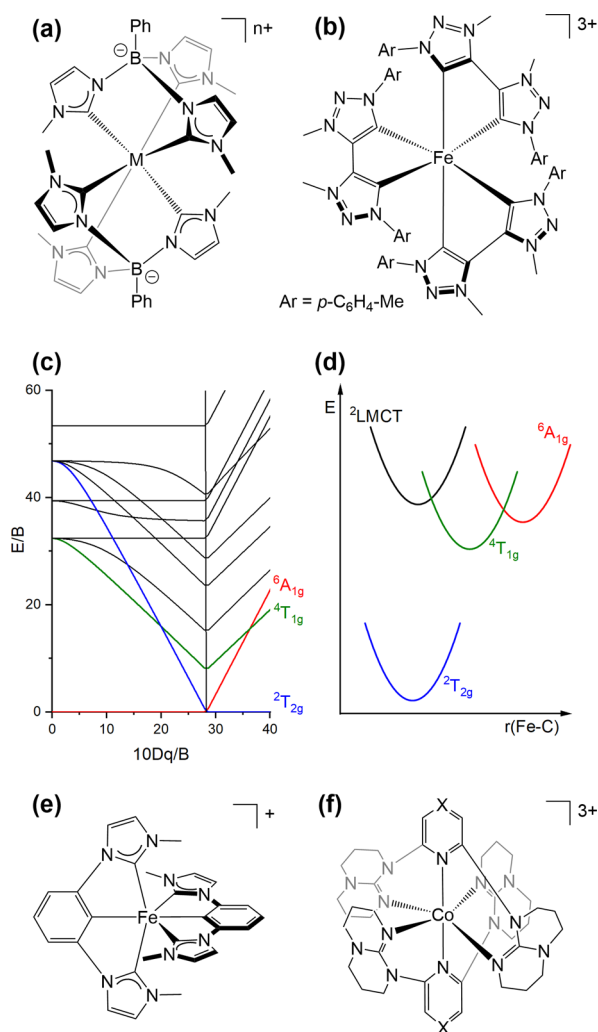


**Figure 5.** Molecular structures of (a)  $[\text{M}(\text{PhB}(\text{MeIm})_3)_2]^{n+}$  (with  $\text{M} = \text{Mn}^{\text{IV}}$ ,  $n = 2$ ;  $\text{M} = \text{Fe}^{\text{III}}$ ,  $n = 1$ ;  $\text{M} = \text{Co}^{\text{III}}$ ,  $n = 1$ )<sup>30,119,149</sup> and (b)  $[\text{Fe}(\text{btz})_3]^{3+}$ .<sup>29</sup> (c) Tanabe–Sugano diagram for the  $d^5$  electron configuration in an octahedral ligand field. (d) Single configurational coordinate diagram with key electronic states in  $[\text{Fe}(\text{btz})_3]^{3+}$ .<sup>29</sup> Molecular structures of (e)  $[\text{Fe}(\text{Imp})_2]^+$  and (f)  $[\text{Co}(\text{dgpy})_2]^{3+}$  ( $\text{X} = \text{CH}$ ) as well as  $[\text{Co}(\text{dgpz})_2]^{3+}$  ( $\text{X} = \text{N}$ ).<sup>51,52</sup>

5d), which limits the efficiency of direct nonradiative relaxation. Third, although low-lying MC states are considerably distorted with respect to the LMCT, the activation barriers for internal conversion are sizable (4–22 kJ/mol), and consequently nonradiative relaxation via the MC states is not ultrafast, but instead permits LMCT luminescence with a lifetime of 100 ps and a quantum yield of  $3 \times 10^{-4}$  at room temperature (Table 1).

In a follow-up study, the energies of the low-lying  $^4\text{MC}$  and  $^6\text{MC}$  states were further increased by creating an even stronger ligand field with the more  $\sigma$ -donating (anionic)  $\text{PhB}(\text{MeIm})_3$  ligand (Figure 5a,  $\text{M} = \text{Fe}^{\text{III}}$ ,  $n = 1$ ).<sup>30</sup> According to an Arrhenius-type analysis, the crossing frequency from the emissive  $^2\text{LMCT}$  to the dark  $^4\text{MC}$  state in the  $[\text{Fe}(\text{PhB}(\text{MeIm})_3)_2]^+$  complex is reduced by at least an order of magnitude compared to  $[\text{Fe}(\text{btz})_3]^{3+}$ , which is likely of key importance for the observable improved photophysical properties. Though a luminescence quantum yield of 2% and an excited-state lifetime of 2.0 ns may seem low compared to precious metal emitters,<sup>123</sup> these figures of merit are

spectacular for an open-shell first-row transition metal complex (Table 1).

The spin-allowed nature of the relevant LMCT transition is instrumental to make radiative relaxation competitive with nonradiative excited-state deactivation in these Fe<sup>III</sup> compounds, but at the same time this has a detrimental effect on the photoreactivity of the luminescent <sup>2</sup>LMCT state: Though its reductive quenching by sacrificial electron donors is fast, the photoreduction efficiencies are very low (5%), because photogenerated electron–hole pairs rapidly recombine before they are spatially separated into longer-lived reduction and oxidation products.<sup>124</sup> This so-called geminate recombination within the “solvent cage” is a well-known phenomenon, which becomes particularly cumbersome when the electron–hole recombination is spin-allowed (i. e., associated with no net spin change).<sup>125</sup> Unfortunately, this is the case for electron transfer from tertiary amine donors to the <sup>2</sup>LMCT-excited Fe<sup>III</sup> complex, because this yields a low-spin Fe<sup>II</sup> complex (a singlet) and an oxidized amine (a doublet), which can undergo spin-allowed reverse electron transfer to form the Fe<sup>III</sup> complex in its doublet ground state and the neutral amine in its singlet state.<sup>124</sup> In Ru<sup>II</sup> complexes, photoreduction efficiencies are in the range of 5–60%, indicating that this is a general problem, which does however diminish when the electron–hole recombination becomes spin-forbidden.<sup>125</sup>

The [Fe(PhB(MeIm)<sub>3</sub>)<sub>2</sub>]<sup>+</sup> complex furthermore undergoes “self-quenching” in sufficiently concentrated acetonitrile solution (70 mM). In this reaction, the <sup>2</sup>LMCT-excited Fe<sup>III</sup> compound reacts with one equivalent of itself in the electronic ground state, to afford the Fe<sup>II</sup> and Fe<sup>IV</sup> forms of this complex.<sup>126</sup> This is likely the first clear-cut case of photo-induced symmetry-breaking charge separation in a transition metal complex, and it became possible due to the fact that the [Fe(PhB(MeIm)<sub>3</sub>)<sub>2</sub>]<sup>+</sup> complex features three different metal-centered redox processes (without interfering ligand-based redox events). As a consequence, the symmetry-breaking charge separation reaction becomes strongly exergonic, and although geminate in-cage charge recombination is rapid, the Fe<sup>II</sup> and Fe<sup>IV</sup> photoproducts form in 4% yield.

The [Fe(ImP)<sub>2</sub>]<sup>+</sup> complex (Figure 5e) seems to show even more unusual luminescence behavior than the only other two Fe<sup>III</sup> emitters known so far.<sup>51</sup> UV excitation of [Fe(ImP)<sub>2</sub>]<sup>+</sup> in CH<sub>3</sub>CN is thought to populate a “hot” <sup>2</sup>MLCT excited state, from which a branching into the relaxed <sup>2</sup>MLCT and a lower-lying <sup>2</sup>LMCT states occurs. Strikingly, both of these states seem to be luminescent (Table 1), one at 450 nm and the other at 675 nm, with lifetimes of 4.2 and 0.2 ns, respectively.

The photophysical properties of the [Co(dgpy)<sub>2</sub>]<sup>3+</sup> and [Co(dgpz)<sub>2</sub>]<sup>3+</sup> complexes (Figure 5f) are comparatively easy to rationalize.<sup>52</sup> Both complexes emit blue-green with nanosecond lifetime in acetonitrile at room temperature and luminescence quantum yields of 0.4–0.7% (Table 1). The combination of relatively electron-rich ligands with a metal trication leads to a charge transfer reversal with respect to classical Fe<sup>II</sup> polypyridines,<sup>127,128</sup> and the emissive excited state has <sup>3</sup>LMCT character. The large bite angle of the dgpy and dgpz ligands (in particular when compared to tpy as a prototypical terdentate ligand in photoactive metal complexes)<sup>129</sup> likely plays a key role in establishing a sufficiently strong ligand field to shift MC states to high energies and to decelerate <sup>3</sup>LMCT deactivation via such MC states. In this sense, the molecular design of [Co(dgpy)<sub>2</sub>]<sup>3+</sup> and [Co(dgpz)<sub>2</sub>]<sup>3+</sup> takes some of the lessons learned about the

importance of bite angle optimization in Fe<sup>II</sup> and Cr<sup>III</sup> complexes into account.<sup>130,131</sup>

## 5. MC EMITTERS: 3d<sup>2</sup> (V<sup>III</sup>), 3d<sup>3</sup> (Cr<sup>III</sup>, Mn<sup>IV</sup>), AND 3d<sup>6</sup> (Co<sup>III</sup>) COMPLEXES

Spin-flip transitions within a given d<sup>n</sup> electron configuration (*n* = 2–8) typically give rise to excited states that are only weakly distorted relative to the ground state, because they usually do not lead to significant changes of the metal–ligand bonding situation, and this is beneficial to decelerate nonradiative deactivation. For octahedrally coordinated d<sup>2</sup> and d<sup>3</sup> complexes such spin-flips are expected as lowest excited states in sufficiently strong ligand fields (Figure 6a/b). Doped into inorganic host materials, d<sup>2</sup> and d<sup>3</sup> ions have long been known to emit from the respective spin-flip excited states,<sup>132</sup> and some molecular Cr<sup>III</sup> complexes were shown to luminesce in solution at room temperature, though until recently mostly with very low quantum yields.<sup>133</sup>

The field of luminescent Cr<sup>III</sup> complexes recently experienced a strong revival, initiated by the discovery of the exceptional photophysical properties of [Cr(ddpd)<sub>2</sub>]<sup>3+</sup> (Figure 6c, M = Cr).<sup>131</sup> Compared to other tridentate ligands such as tpy, the ddpd ligand offers a larger bite angle that causes a stronger ligand field as a result of better overlap between metal 3d- and ligand-orbitals. This is helpful, because it widens the energy gap between the emissive <sup>2</sup>E<sub>g</sub> and the higher-lying <sup>4</sup>T<sub>2</sub> state (blue and orange in Figure 6b, respectively), leading to a smaller thermal population of the latter via reverse intersystem crossing and limiting nonradiative relaxation from this strongly distorted excited state. Further optimizations were possible by ligand deuteration, which decelerates unwanted nonradiative processes and thereby leads to a luminescence quantum yield of 30% paired with a <sup>2</sup>E lifetime of 2.3 ms in solution at room temperature (Table 2).<sup>134</sup> Applications in temperature<sup>135</sup> and pressure sensing were possible,<sup>136</sup> and the singlet oxygen sensitization capability of [Cr(ddpd)<sub>2</sub>]<sup>3+</sup> was exploited for photocatalysis.<sup>137</sup> Much of this work has been reviewed.<sup>22,138,139</sup>

In a very recent study, the NMe bridging units of ddpd were replaced by –CH<sub>2</sub>– groups (Figure 6d), which induces a blue-shift of the emission band maximum from 775 nm in [Cr(ddpd)<sub>2</sub>]<sup>3+</sup> to 709 nm in the new [Cr(bpmp)<sub>2</sub>]<sup>3+</sup> complex.<sup>140</sup> As the <sup>2</sup>E energy depends essentially on the repulsion between metal d-electrons, this experimental observation suggests that the extent of metal–ligand bond covalence is different in [Cr(bpmp)<sub>2</sub>]<sup>3+</sup> than in [Cr(ddpd)<sub>2</sub>]<sup>3+</sup>. Curiously, analysis of the spectroscopic properties of [Cr(bpmp)<sub>2</sub>]<sup>3+</sup> in terms of ligand field theory yielded a Racah B parameter of 1003 cm<sup>−1</sup>, which is higher than the B-value for the free Cr<sup>III</sup> ion in the gas phase (918 cm<sup>−1</sup>) and substantially larger than the Racah B parameter determined for [Cr(dqp)<sub>2</sub>]<sup>3+</sup> (656 cm<sup>−1</sup>).<sup>141,142</sup> The new complex furthermore has a high luminescence quantum yield (20%), and it was noted that [Cr(bpmp)<sub>2</sub>]<sup>3+</sup> surpasses [Ru(bpy)<sub>3</sub>]<sup>2+</sup>, though spin-flip emission from a very weakly distorted MC excited state and luminescence from an MLCT state are two very different things. The comparison to an europium(III)-based emitter also made in the respective study seems more appropriate, because that compound's emissive MC state is likely more similarly weakly distorted as the luminescent (spin-flip) MC state of [Cr(bpmp)<sub>2</sub>]<sup>3+</sup>.

The dqp ligand was known from previous work with Ru<sup>II</sup><sup>143</sup> and recently turned out to be applicable in Cr<sup>III</sup> coordination

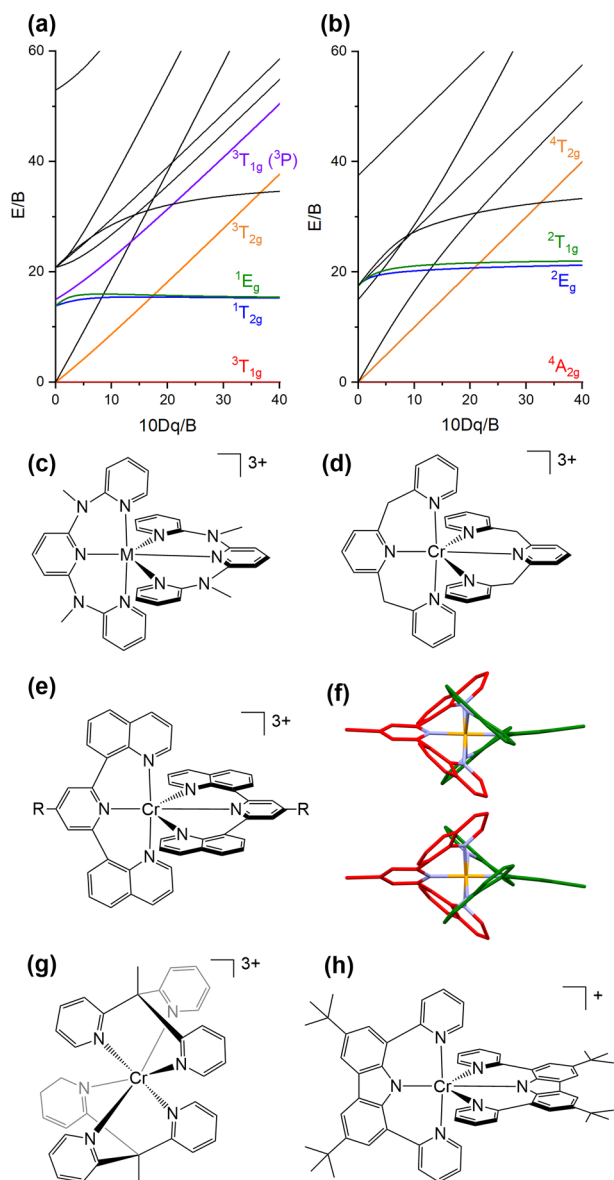


**Figure 6.** Tanabe–Sugano diagrams for the  $d^2$  (a) and the  $d^3$  (b) electron configurations in an octahedral ligand field. (c) Molecular structure of  $[M(\text{ddpd})_2]^{3+}$ ;  $M = \text{Cr}^{\text{III}}$  or  $\text{V}^{\text{III}}$ .<sup>34,131,134–137,139</sup> (d) Molecular structure of  $[\text{Cr}(\text{bpmp})_2]^{3+}$ .<sup>140</sup> (e) Molecular structure of  $[\text{Cr}(\text{Rdqp})_2]^{3+}$ , where  $R = \text{H}$ ,  $\text{OMe}$ ,  $\text{Br}$  or  $\text{C}\equiv\text{CH}$ .<sup>142,144,145</sup> (f) Enantiomeric pair  $PP$ - $[\text{Cr}(\text{Brdqp})_2]^{3+}$  (upper) and  $MM$ - $[\text{Cr}(\text{Brdqp})_2]^{3+}$  (lower). The  $\text{Cr}^{\text{III}}$  ion is orange, N atoms are blue, and the two  $\text{Brdqp}$  ligands are in red and green, respectively.<sup>145</sup> (g) Molecular structure of  $[\text{Cr}(\text{tpe})_2]^{3+}$ .<sup>147</sup> (h) Molecular structure of  $[\text{Cr}(\text{dpc})_2]^+$ .<sup>148</sup>

chemistry as well.<sup>142</sup> The development of a new synthetic strategy gave access to heteroleptic  $\text{Cr}^{\text{III}}$  compounds, in which  $\text{ddpd}$ ,  $\text{dpq}$ , and  $\text{tpy}$  (as well as substituted variants thereof) were combined (Table 2). In the homoleptic  $[\text{Cr}(\text{dqp})_2]^{3+}$  complex (Figure 6e), the two meridionally coordinating  $\text{dqp}$  ligands wrap around each other to result in a helical conformation around a pseudo- $C_2$  axis, stabilized by intramolecular  $\pi$ -stacking interactions (Figure 6f).<sup>144</sup> The complexation reaction leads exclusively to the  $PP$ - $[\text{Cr}(\text{dqp})_2]^{3+}$  and  $MM$ - $[\text{Cr}(\text{dqp})_2]^{3+}$  pair of enantiomers, while the  $PM$  diastereomer is not formed. No racemization was observed over several months and the absolute configurations of the two

enantiomers were determined.  $PP$ - $[\text{Cr}(\text{dqp})_2]^{3+}$  and  $MM$ - $[\text{Cr}(\text{dqp})_2]^{3+}$  show circularly polarized luminescence (CPL) with dissymmetry factors ( $g_{\text{lum}}$ ) that surpass those for previously reported d-metal complexes by at least an order of magnitude,<sup>144</sup> owing to the fact that the two relevant emission spin-flip transitions ( ${}^2E \rightarrow {}^4A_2$  and  ${}^2T_1 \rightarrow {}^4A_2$ ) have magnetic-dipole allowed and electric-dipole forbidden character. For transitions of this type,  $g_{\text{lum}}$  theoretically maximizes to values of  $-2$  or  $+2$  when either pure right- or left-handed polarized light is emitted.<sup>145</sup>  $[\text{Cr}(\text{dqp})_2]^{3+}$  in  $\text{CH}_3\text{CN}$  gave  $|g_{\text{lum}}| = 0.2$  for the  ${}^2E$  emission at 749 nm,<sup>144</sup> and nearly equally high values were obtained for three congeners with modified  $\text{dqp}$  ligands (Table 2).<sup>145</sup> The functionalization of  $\text{dqp}$  with a methoxy-group at the central pyridine ring improved the chiral resolution and allowed for a larger scale preparation of the  $[\text{Cr}(\text{OMe}^{\text{dqp}})_2]^{3+}$  luminophore with an emission quantum yield of 17% and an excited-state lifetime of up to 1.35 ms at room temperature in aqueous solution.<sup>145</sup> Similar CPL studies were performed with  $[\text{Cr}(\text{ddpd})_2]^{3+}$ , for which the chiral resolution of  $PP$ - and  $MM$ -enantiomers proved more difficult, and a somewhat lower  $g_{\text{lum}}$  value of  $-0.093$  was found, yet this performance factor remains competitive with many lanthanoid-based CPL emitters.<sup>150</sup>

The  $\text{ddpd}$  and  $\text{dqp}$  ligands preferentially coordinate  $\text{Cr}^{\text{III}}$  in a meridional fashion (though facially coordinated  $\text{dqp}$  complexes of  $\text{Ru}^{\text{II}}$  are known);<sup>151</sup> hence, no inversion center is present in these complexes and the parity selection rule for d–d transitions does not hold true in a strict sense. In the  $[\text{Cr}(\text{tpe})_2]^{3+}$  complex (Figure 6g), the tridentate ligand is forced to coordinate facially, which installs an inversion center and renders the  ${}^2E_g \rightarrow {}^4A_{2g}$  luminescence transition Laporte-forbidden.<sup>147</sup> The radiative  ${}^2E$  decay rate is therefore only on the order of  $20 \text{ s}^{-1}$ , similarly low as in centrosymmetric  $[\text{Cr}(\text{CN})_6]^{3-}$ .<sup>146</sup> Since nonradiative relaxation pathways remain moderately efficient also in  $[\text{Cr}(\text{tpe})_2]^{3+}$ , the new design principle resulted in an exceptionally long luminescence lifetime of 4.5 ms in aqueous solution at room temperature.

The  $\text{Cr}^{\text{III}}$  polypyridine complexes known until very recently all had their emission band maxima in the rather narrow spectral range between 709 and 778 nm. The  $[\text{Cr}(\text{dpc})_2]^+$  complex (Figure 6h) is the first near-infrared-II emitter in this compound family, featuring an emission band maximum at 1067 nm in frozen  $\text{CH}_3\text{CN}$  at 77 K.<sup>148</sup> This drastic red-shift seems to be the result of increased metal–ligand bond covalence achievable by the mixed amido and pyridine coordination environment. This design principle of exploiting the nephelauxetic effect, which operates particularly well on intraconfigurational (spin-flip) states, is radically different from the common approach of enhancing the ligand field strength, which is typically applied to modulate the energies of interconfigurational states.

While many molecular  $\text{Cr}^{\text{III}}$  complexes are emissive from their  ${}^2E$  state,<sup>152</sup> currently it seems that there exists only one example of an isoelectronic molecular  $\text{Mn}^{\text{IV}}$  compound showing the same type of photoluminescence.<sup>119</sup> Specifically, the  $[\text{Mn}(\text{PhB}(\text{MeIm})_3)_2](\text{OTf})_2$  complex (Figure 5a,  $M = \text{Mn}^{\text{IV}}$ ,  $n = 2$ ) reported in section 4 shows visible LMCT emission alongside NIR  ${}^2E \rightarrow {}^4A_2$  luminescence with a band maximum at 814 nm in the solid state (Table 2). This is significantly red-shifted compared to most of the molecular  $\text{Cr}^{\text{III}}$  complexes and likely reflects a high degree of metal–ligand bond covalence in this  $\text{Mn}^{\text{IV}}$  complex.<sup>119</sup> Presumably, the higher metal oxidation state leads to a stronger



**Table 2. Complexes Emitting from Metal-Centered Excited States and Some of Their Key Photophysical Properties in Deaerated Solution at Room Temperature**

compd	electron configuration	solvent	$\lambda_{em}$ [nm]	$\tau_0$	$\phi$ [%]	type of emission	ref
<i>mer</i> -[V(ddpd) <sub>2</sub> ] <sup>3+</sup>	d <sup>2</sup>	CD <sub>3</sub> CN	396	5.4 ns <sup>a</sup>	2.1	MC/LMCT	34
			1109/1123	1.35 $\mu$ s <sup>b</sup>	0.00018	MC	34
[VCl <sub>3</sub> (ddpd)]	d <sup>2</sup>	solid state	1102/1219/1256 <sup>c</sup>	0.5 $\mu$ s <sup>c</sup>		MC	33
[Cr(CN) <sub>6</sub> ] <sup>3-</sup>	d <sup>3</sup>	H <sub>2</sub> O	<sup>d</sup>	0.12 $\mu$ s		MC	146
<i>fac</i> -[Cr(tpc) <sub>2</sub> ] <sup>3+</sup>	d <sup>3</sup>	D <sub>2</sub> O/DCIO <sub>4</sub>	748	4.5 ms	8.2	MC	147
<i>mer</i> -[Cr(D <sub>9</sub> -ddpd) <sub>2</sub> ] <sup>3+</sup>	d <sup>3</sup>	CD <sub>3</sub> CN	738/778	2.3 ms	30.1	MC	134
<i>mer</i> -[Cr(bpmp) <sub>2</sub> ] <sup>3+</sup>	d <sup>3</sup>	D <sub>2</sub> O/DCIO <sub>4</sub>	709	1.8 ms	19.6	MC	140
[Cr(dpq) <sub>2</sub> ] <sup>3+</sup>	d <sup>3</sup>	H <sub>2</sub> O	724/747	1.2 ms	5.2	MC	144
[Cr(dqp)(tpy)] <sup>3+</sup>	d <sup>3</sup>	CH <sub>3</sub> CN	724/746	578 $\mu$ s	0.2	MC	142
[Cr(ddpd)(dqp)] <sup>3+</sup>	d <sup>3</sup>	CH <sub>3</sub> CN	728/762	642 $\mu$ s	6.0	MC	142
[Cr(dqp)( <sup>OMe</sup> dqp)] <sup>3+</sup>	d <sup>3</sup>	CH <sub>3</sub> CN	725/752	855 $\mu$ s	6.5	MC	142
[Cr( <sup>OMe</sup> dqp) <sub>2</sub> ] <sup>3+</sup>	d <sup>3</sup>	H <sub>2</sub> O	720/756	1.35 ms	17	MC	145
[Cr(dpc) <sub>2</sub> ] <sup>+</sup>	d <sup>3</sup>	CH <sub>3</sub> CN <sup>e</sup>	1067 <sup>e</sup>	2.0 $\mu$ s <sup>f</sup>	<0.00089 <sup>e</sup>	MC	148
[Mn(PhB(MeIm) <sub>3</sub> ) <sub>2</sub> ](OTf) <sub>2</sub>	d <sup>3</sup>	solid state	815 <sup>g</sup>	1.5 $\mu$ s <sup>g</sup>		MC	119
			600	50 ns		LMCT	
[Co(CN) <sub>6</sub> ] <sup>3-</sup>	d <sup>6</sup>	H <sub>2</sub> O	726 <sup>h</sup>	2.6 ns		MC	28, 146
[Co(PhB(MeIm) <sub>3</sub> ) <sub>2</sub> ] <sup>+</sup>	d <sup>6</sup>	CH <sub>3</sub> CN	690	0.82 $\mu$ s	0.01	MC	149

<sup>a</sup>Weighted average from a biexponential decay fit (3.2 ns (56%), 8.2 ns (44%)). <sup>b</sup>Weighted average from a biexponential decay fit (790 ns (93%), 8800 ns (7%)), measured at 77 K in <sup>n</sup>BuCN. <sup>c</sup>Data obtained in the solid state at 298 K. <sup>d</sup>No emission maximum was reported in the original work. <sup>e</sup>Measured at 77 K. <sup>f</sup>Weighted average from a biexponential decay fit (1.4  $\mu$ s (88%), 6.3  $\mu$ s (12%)), measured at 77 K. <sup>g</sup>Data obtained in the solid state at 77 K. <sup>h</sup>Measured in an ethylene glycol/water mixture (60/40 vol %) at 165 K.

nephelauxetic effect, decreasing the mutual repulsion between d-electrons and lowering the energy of the emissive <sup>2</sup>E state.

Taking a leftward step from Cr<sup>III</sup> in the periodic table, the d<sup>3</sup> valence electron configuration is achievable with V<sup>II</sup>, for example in [V(bpy)<sub>3</sub>]<sup>2+</sup> and [V(phen)<sub>3</sub>]<sup>2+</sup>. These compounds have low-lying <sup>2</sup>MLCT states that mix with the lowest metal-centered doublet states.<sup>153,154</sup> This produces geometric distortion and energetic stabilization, causing efficient non-radiative relaxation. The finding that a <sup>2</sup>MLCT state is at lower energy than the corresponding <sup>4</sup>MLCT implies that Hund's rule is not necessarily obeyed in cases with substantial overlap between singly occupied ligand- and metal-centered orbitals. It seems plausible that the use of bpy and phen ligands with electron-donating ligands will elevate the MLCT energies to the extent that <sup>2</sup>E emission will become observable.<sup>153</sup>

As noted above, aside from the d<sup>3</sup> valence electron configuration, octahedral d<sup>2</sup> complexes are obvious candidates for a spin-flip as lowest-lying excited state (Figure 6a), but until recently no molecular complexes of this type have been shown to emit in solution. The [V(ddpd)<sub>2</sub>]<sup>3+</sup> complex (Figure 6c, M = V) features <sup>1</sup>E<sub>g</sub>/<sup>1</sup>T<sub>2g</sub> → <sup>3</sup>T<sub>1g</sub> emission around 1100 nm with 1.8 × 10<sup>-4</sup> % quantum yield in CH<sub>3</sub>CN at room temperature, representing the first case of NIR-II emission by a 3d-metal complex in fluid solution.<sup>34</sup> The second overtone of aromatic C–H vibrations has significant spectral overlap with this emission, yet 17-fold deuteration of the ddpd ligand had no clear effect on the luminescence quantum yield, hence the nonradiative decay path could not be unraveled on this basis. The most striking observation was the appearance of blue fluorescence with a quantum yield of 2.1% upon UV excitation. Higher excited-state emission from MC states had been previously reported for d<sup>2</sup> species, but only at cryogenic temperatures.<sup>155</sup> In [V(ddpd)<sub>2</sub>]<sup>3+</sup> this emission was tentatively attributed to the <sup>3</sup>T<sub>1g</sub> (<sup>3</sup>P) → <sup>3</sup>T<sub>1g</sub> transition (purple and red in Figure 6a, respectively) or to <sup>3</sup>LMCT transitions.<sup>34</sup> Though there is a large energy gap of ca. 2 eV between the two emissive excited states, there are several other excited states in between,

and it seems that intersystem crossing from the higher-lying triplet states to the singlets is comparatively inefficient.

The complex [VCl<sub>3</sub>(dppd)] likewise emits from the <sup>1</sup>E<sub>g</sub>/<sup>1</sup>T<sub>2g</sub> manifold but seemingly only in the solid state.<sup>33</sup> Unlike in the homoleptic [V(ddpd)<sub>2</sub>]<sup>3+</sup> congener, excited-state relaxation is strongly susceptible to ligand deuteration, confirming that multiphonon relaxation involving C–H oscillators is a major decay pathway. The large splitting of the electronic ground state, manifesting in the appearance of multiple <sup>1</sup>E<sub>g</sub>/<sup>1</sup>T<sub>2g</sub> → <sup>3</sup>T<sub>1g</sub> emission band maxima, likely further facilitates non-radiative excited-state relaxation by reducing the relevant energy gap. Though vanadium has a very low spin–orbit coupling constant, the rate of intersystem crossing following excitation into singlet states is very high ( $k_{ISC} = 6.7 \times 10^{11} \text{ s}^{-1}$ ), and trajectory surface hopping simulations rationalized that finding.<sup>156</sup> This resonates with a previous study, which found no direct correlation between the magnitude of the spin–orbit coupling constant and the rate for intersystem crossing.<sup>157</sup> Complexation of the V<sup>3+</sup> ion to the ligands (C<sub>6</sub>F<sub>5</sub>)<sub>3</sub>tren and CN<sup>t</sup>Bu resulted in the trigonal bipyramidal complex [V-[(C<sub>6</sub>F<sub>5</sub>)<sub>3</sub>tren](CN<sup>t</sup>Bu)] with a <sup>3</sup>A ground state, and the lowest lying excited state is a <sup>1</sup>E state due to the strong ligand field.<sup>158</sup> The <sup>1</sup>E → <sup>3</sup>A transition is an intraconfigurational, spin-flip transition, which radiates in the near-infrared, however only in frozen matrices at 77 K. Cocrystallization of the V<sup>3+</sup> ion with the diamagnetic analogue Ga<sup>3+</sup> ion afforded [V<sub>0.023</sub>Ga<sub>0.977</sub>[(C<sub>6</sub>F<sub>5</sub>)<sub>3</sub>tren](CN<sup>t</sup>Bu)], for which single crystals were luminescent at room temperature.

[Co(CN)<sub>6</sub>]<sup>3-</sup> is a rare (and long known) example of a 3d<sup>6</sup> complex that emits from a strongly distorted MC state in solution at room temperature.<sup>28,146</sup> With the PhB(MeIm)<sub>3</sub> ligand, it was now possible to create a similarly strong ligand field as with CN<sup>-</sup> (10 Dq = 38 600 cm<sup>-1</sup>), making the [Co(PhB(MeIm)<sub>3</sub>)<sub>2</sub>]<sup>+</sup> complex (Figure 5a, M = Co<sup>III</sup>, n = 1) an MC emitter with a microsecond lifetime in CH<sub>3</sub>CN at room temperature (Table 2).<sup>149</sup> Excitation has to occur into charge-transfer bands in the UV, from which the emissive <sup>3</sup>T<sub>1g</sub> state is

populated via internal conversion and intersystem crossing. While that  $^3T_{1g}$  state is highly problematic for obtaining MLCT emission from  $Fe^{II}$  complexes (because it depopulates the MLCT and rapidly decays via nonradiative relaxation, Figure 4a/b),<sup>66</sup> in the cobalt complex, here this state maintains a sizable energy gap to the ground state even in its relaxed geometry, owing to the strong ligand field.<sup>149</sup> The emission is spin-forbidden and therefore associated with a comparatively low radiative rate constant, which makes nonradiative relaxation very competitive despite the large energy gap. Consequently, the emission quantum yield at room temperature is only 0.01%. Since the  $\sigma$ - and  $\pi$ -bonding properties of the PhB(MeIm)<sub>3</sub> scorpionate ligand can in principle be tuned, this opens the perspective to further enhance the photophysical properties of  $Co^{III}$ -based  $^3T_{1g}$  emitters.

## 6. SUMMARY AND OUTLOOK

Traditional luminophores made from precious  $d^6$  or  $d^8$  metals such as  $Ru^{II}$ ,  $Os^{II}$ ,  $Re^I$ ,  $Ir^{III}$ ,  $Pt^{II}$ , and  $Au^{III}$  typically function on the basis of MLCT (or the closely related MMLCT) transitions.<sup>63,64</sup> Using the less noble element copper in its +I oxidation state with its completely filled  $d^{10}$  subshell, this photophysical behavior was emulated already nearly 40 years ago.<sup>25</sup> The absence of low-lying MC states in the  $d^{10}$  valence electron configuration greatly facilitated this early discovery, and nowadays four-coordinate  $Cu^I$  MLCT emitters are a highly developed compound class.<sup>19,36,57</sup> With the open-shell  $3d^6$  and  $3d^8$  configurations, emissive MLCT excited states are much harder to install, because nonradiative relaxation via low-lying MC states tends to be ultrafast. Until now, most efforts to obtain  $3d^6$  MLCT emitters have concentrated on  $Fe^{II}$  complexes, but despite considerable recent progress in enhancing their MLCT lifetimes and in understanding their electronic structures no  $Fe^{II}$  based MLCT luminophores are yet known.<sup>66–68,72–74,77,78,120–122</sup> Very recently, complexes of isoelectronic  $Cr^0$  and  $Mn^I$  have been identified as  $3d^6$  MLCT emitters showing analogous photophysical and photochemical behavior as  $Ru^{II}$  polypyridines or cyclometalated  $Ir^{III}$  complexes (Figure 7a).<sup>32,46,47,159,160</sup> In parallel, considerable progress has been made toward  $3d^8$  MLCT luminophores based on  $Ni^{II}$ , though in this case the breakthrough has not yet been made in the sense that room-temperature MLCT emission has not been achievable until now.<sup>49,109</sup>

A paradigm change occurred with the recent emergence of highly emissive two-coordinate  $Cu^I$  complexes which are LLCT luminophores (Figure 7b),<sup>37–39,42,45</sup> and with the discovery of  $Mn^{IV}$  and  $Fe^{III}$  LMCT emitters (Figure 7a).<sup>29,30,119</sup> The reversal of the charge transfer direction when going from MLCT to LMCT has direct consequences for possible applications in dye-sensitized solar cells;<sup>161</sup> yet as far as the luminescence properties are concerned, LMCT or LLCT emitters seem highly competitive with MLCT luminophores.<sup>87,127</sup> This is particularly true for the new class of linear  $Cu^I$  LLCT emitters,<sup>37–39,42,45</sup> which represents a conceptual breakthrough in the photophysics of copper(I) after a long period with a dominant focus on tetrahedral  $Cu^I$  MLCT luminophores.<sup>36</sup> The  $Fe^{III}$  LMCT emitters reported so far exhibit spin-allowed luminescence,<sup>29,30,51,124</sup> which is helpful to boost luminescence quantum yields because it makes radiative relaxation kinetically more competitive with nonradiative processes. On the other hand, the spin-allowed character of the photoactive excited state is likely disadvantageous for some photochemical applications, because spin-

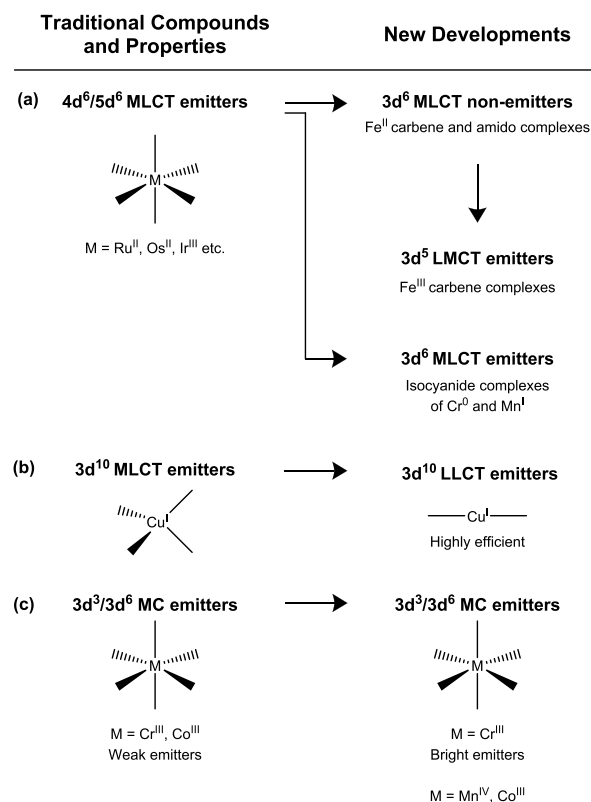


Figure 7. Recent key developments summarized graphically.

allowed geminate charge recombination is expected to hamper cage-escape yields,<sup>13,124</sup> thereby perhaps limiting the effectiveness of these sensitizers for photoinduced electron transfer.

Analogously to the LMCT emitters made from  $Fe^{III}$  and  $Mn^{IV}$ , new MC luminophores based on  $Cr^{III}$  and  $V^{III}$  do not have diamagnetic ground states, which represents another key difference to the traditional  $d^6$  and  $d^{10}$  MLCT luminophores. In the case of  $Cr^{III}$  this leads to the well-known ruby-like emission that has been optimized and brought to new applications in recent years (Figure 7c),<sup>131,134–139,142,144,145,147,148,150,162</sup> whereas in the case of  $V^{III}$  an analogous spin-flip transition has now become emissive in a molecular complex.<sup>34</sup> Similarly to the  $Cr^{III}$  emitters reported recently, a new  $Co^{III}$  based MC luminophore outperforms an earlier investigated analogue and benefits from new insights concerning the design of coordination environments to maximize ligand field strength and minimize unwanted nonradiative relaxation processes.<sup>149</sup> The spin-forbidden nature of the MC emissions of these  $d^3$  and  $d^6$  compounds is similar to the traditional  $^3MLCT$  luminescence in  $d^6$  or  $d^{10}$  compounds, though different spin selection rules will apply for energy transfer depending on the exact electron configuration of the reactive excited states.<sup>163</sup> This could have important implications in energy transfer catalysis,<sup>164</sup> because not all photocatalyst/substrate combinations will represent equally good donor–acceptor pairs in which energy transfer is equally spin-allowed.

One particularly striking new finding is that several of the newly reported first-row transition metal complexes emit from higher excited states. In the  $Fe^{III}$  carbene complexes, there are two MC states with different spin multiplicities below the emissive  $^2LMCT$  state.<sup>29,30</sup> In the  $Mn^{IV}$  and  $V^{III}$  complexes, it seems possible that their higher excited-state emissions even

originate from states that have the same multiplicity as lower-lying (MC) states<sup>34,119</sup> and as such would represent exceptions to Kasha's rule, according to which typically only the lowest electronically excited state of a given multiplicity emits with appreciable quantum yields.<sup>165</sup> In the solid state at cryogenic temperatures, such behavior has been known for some first-row transition metals (including Ti<sup>2+</sup> and Ni<sup>2+</sup> when doped into halide host matrices),<sup>166</sup> but for molecular compounds at room temperature this is very uncommon behavior.

Decelerating nonradiative excited-state relaxation remains the most challenging part in the development of new emissive metal complexes, particularly in the first row of transition metals, where the ligand field is typically comparatively weak and low-lying MC states can represent effective deactivation channels (Figure 1b).<sup>3,22,23,65,77</sup> There is no single recipe that is uniformly applicable to address this issue in different metals and oxidation states, because each d<sup>n</sup> valence electron configuration has its own characteristics. Fairly general guidelines include however the design of rigid coordination environments to limit vibrational degrees of freedom,<sup>38,39,84,86,87</sup> the enhancement of the ligand field strength to shift MC states to higher energies,<sup>73,77,78,120–122,167</sup> the optimization of coordination geometries to minimize splitting of degenerate states into several sublevels and to maximize energy gaps between individual states,<sup>130,131,138,162</sup> the installment of an inversion center to influence radiative excited-state decay rates,<sup>147</sup> and the introduction of push- and/or pull-character to control the energies of charge-transfer states.<sup>73,168</sup> Perhaps less obvious but potentially interesting could be strategies based on optimizing metal–ligand bond covalence to minimize repulsion between spectroscopically relevant d-orbitals<sup>148</sup> as well as the exploitation of triplet reservoir and/or delocalization effects<sup>47</sup> in first-row transition metal-based compounds with covalently attached organic chromophores.<sup>92–94</sup> Ligand deuteration, a well-known strategy in the field of lanthanide luminophores, is now successfully applied to first-row transition metal emitters.<sup>134</sup>

Aside from the broadened perspectives with regard to the accessible emission types (including LMCT and LLCT in addition to the traditionally explored MLCT and MC transitions), there are very important recent developments beyond the first-row of transition metals. On the one hand, this includes comparatively abundant second- and third-row transition metals (for example Zr,<sup>87,116</sup> Mo,<sup>83,84,95,160</sup> or W<sup>82,95,160,169,170</sup>) or f-elements (for example Ce<sup>171,172</sup>). On the other hand, molecular complexes of abundant main group elements are now attracting increasing attention as luminophores and provide additional insight into how nonradiative relaxation can be tamed.<sup>173–175</sup> At the same time, further developments of precious metal-based complexes (for example, Ru,<sup>167,176,177</sup> Rh,<sup>178,179</sup> Re,<sup>180–182</sup> Ir,<sup>183–185</sup> or Pt<sup>186–188</sup>) have significantly advanced the field of inorganic photophysics and photochemistry. Regardless of whether complexes of d-, f-, or main group elements are considered, the interplay between synthetic, spectroscopic, and computational work<sup>189</sup> seems crucial for the development of new designer luminophores.

## AUTHOR INFORMATION

### Corresponding Author

Oliver S. Wenger – Department of Chemistry, University of Basel, 4056 Basel, Switzerland; [orcid.org/0000-0002-0739-0553](https://orcid.org/0000-0002-0739-0553); Email: [oliver.wenger@unibas.ch](mailto:oliver.wenger@unibas.ch)

## Author

Christina Wegeberg – Department of Chemistry, University of Basel, 4056 Basel, Switzerland; [orcid.org/0000-0002-6034-453X](https://orcid.org/0000-0002-6034-453X)

Complete contact information is available at: <https://pubs.acs.org/10.1021/jacsau.1c00353>

## Author Contributions

The manuscript was written through contributions of all authors.

## Notes

The authors declare no competing financial interest.

## ACKNOWLEDGMENTS

This work was supported by the Swiss National Science Foundation through grant number 200021\_178760. C. W. thanks the Independent Research Fund Denmark for an international postdoctoral grant (9059-00003B).

## ABBREVIATIONS

bpmp, 2,6-bis(2-pyridinmethyl)pyridine; bpy, 2,2'-bipyridine; btz, 3,3'-dimethyl-1,1'-bis(*p*-tolyl)-4,4'-bis(1,2,3-triazol-5-ylidene)); CAAC, cyclic (alkyl)(amino)carbene; Cp, cyclopentadienyl anion; Cp\*, pentamethylcyclopentadienyl anion; CPL, circularly polarized luminescence; Cz, carbazolyl; DAC\*, diamidocarbene; ddpd, *N,N'*-dimethyl-*N,N'*-dipyridine-2-ylpyridine-2,6-diamine); dgpy, 1,3-bis(3,4,7,8-tetrahydro-2*H*-pyrimido[1,2-*a*]pyrimidin-1(6*H*)-yl)benzene); dgpz, 3,5-bis(3,4,7,8-tetrahydro-2*H*-pyrimido[1,2-*a*]pyrimidin-1(6*H*)-yl)pyridine); dipp, 2,6-diisopropylphenyl; dpb, 1,3-di(pyridine-2-yl)benzene; dqp, 2,6-di(quinolin-8-yl)pyridine); dpc, 3,6-di-*tert*-butyl-1,8-di(pyridine-2-yl)-carbazole; <sup>OMe</sup>dqp, 2,6-di(quinolin-8-yl)-4-methoxy-pyridine); GS, ground state; HBUImP, 1,1'-(1,3-phenylene)bis(3-butyl-1-imidazol-2-ylidene); HIMP, 1,1'-(1,3-phenylene)bis(3-methyl-1-imidazol-2-ylidene); HOMO, highest occupied molecular orbital; ISC, intersystem crossing; L<sup>bi</sup>, 2,5-bis(3,5-di-*tert*-butyl-2-isocyanophenyl)thiophene; LLCT, ligand-to-ligand charge transfer; LMCT, ligand-to-metal charge transfer; L<sup>tBu</sup>, 3,3'',5,5''-tetra-*tert*-butyl-2,2''-diisocyno-1,1':3',1''-terphenyl; L<sup>tri</sup>, 5,5'-(2-isocyno-5-methyl-1,3-phenylene)bis(2-(3,5-di-*tert*-butyl-2-isocyanophenyl)-thiophene); LUMO, lowest unoccupied molecular orbital; MAC\*, monoamido-aminocarbene; MC, metal-centered; MLCT, metal-to-ligand charge transfer; MMLCT, metal–metal-to-ligand charge transfer; OTf, triflate; PhB(MeIm)<sub>3</sub>, tris(3-methylimidazolin-2-ylidene)(phenyl)borate; phen, 1,10-phenanthroline); RISC, reverse intersystem crossing; TADF, thermally activated delayed fluorescence; TD-DFT, time-dependent density functional theory; tpe, 1,1,1-tris(pyrid-2-yl)ethane); tpy, 2,2';6',2''-terpyridine); tren = tris(2-aminoethyl)amine

## REFERENCES

- Balzani, V.; Campagna, S. *Photochemistry and Photophysics of Coordination Compounds I*. Springer: Berlin, Heidelberg, New York, 2007.
- Balzani, V.; Campagna, S. *Photochemistry and Photophysics of Coordination Compounds II*. Springer: Berlin, Heidelberg, New York, 2007.
- McCusker, J. K. Electronic structure in the transition metal block and its implications for light harvesting. *Science* **2019**, *363*, 484–488.

- (4) Ford, P. C. From curiosity to applications. A personal perspective on inorganic photochemistry. *Chem. Sci.* **2016**, *7*, 2964–2986.
- (5) Hauser, A.; Reber, C. Spectroscopy and Chemical Bonding in Transition Metal Complexes. *Struct. Bonding (Berlin, Ger.)* **2016**, *172*, 291–312.
- (6) Caspar, J. V.; Kober, E. M.; Sullivan, B. P.; Meyer, T. J. Application of the energy gap law to the decay of charge-transfer excited states. *J. Am. Chem. Soc.* **1982**, *104*, 630–632.
- (7) Prier, C. K.; Rankic, D. A.; MacMillan, D. W. C. Visible Light Photoredox Catalysis with Transition Metal Complexes: Applications in Organic Synthesis. *Chem. Rev.* **2013**, *113*, 5322–5363.
- (8) Yoon, T. P.; Ischay, M. A.; Du, J. N. Visible Light Photocatalysis as a Greener Approach to Photochemical Synthesis. *Nat. Chem.* **2010**, *2*, 527–532.
- (9) Ardo, S.; Meyer, G. J. Photodriven heterogeneous charge transfer with transition-metal compounds anchored to TiO<sub>2</sub> semiconductor surfaces. *Chem. Soc. Rev.* **2009**, *38*, 115–164.
- (10) Li, L.-K.; Tang, M.-C.; Lai, S.-L.; Ng, M.; Kwok, W.-K.; Chan, M.-Y.; Yam, V. W.-W. Strategies towards rational design of gold(III) complexes for high-performance organic light-emitting devices. *Nat. Photonics* **2019**, *13*, 185–191.
- (11) Yersin, H.; Rausch, A. F.; Czerwieńiec, R.; Hofbeck, T.; Fischer, T. The Triplet State of Organo-Transition Metal Compounds. Triplet Harvesting and Singlet Harvesting for Efficient OLEDs. *Coord. Chem. Rev.* **2011**, *255*, 2622–2652.
- (12) Montalti, M.; Credi, A.; Prodi, L.; Gandolfi, M. T. *Handbook of Photochemistry*; CRC Taylor & Francis: Boca Raton, FL, 2006.
- (13) Olmsted, J.; Meyer, T. J. Factors Affecting Cage Escape Yields Following Electron-Transfer Quenching. *J. Phys. Chem.* **1987**, *91*, 1649–1655.
- (14) Bizzarri, C.; Spuling, E.; Knoll, D. M.; Volz, D.; Bräse, S. Sustainable metal complexes for organic light-emitting diodes (OLEDs). *Coord. Chem. Rev.* **2018**, *373*, 49–82.
- (15) Costa, R. D.; Orti, E.; Bolink, H. J.; Monti, F.; Accorsi, G.; Armaroli, N. Luminescent ionic transition-metal complexes for light-emitting electrochemical cells. *Angew. Chem., Int. Ed.* **2012**, *51*, 8178–8211.
- (16) Henwood, A. F.; Zysman-Colman, E. Luminescent Iridium Complexes Used in Light-Emitting Electrochemical Cells (LEECs). *Top. Curr. Chem.* **2016**, *374*, 36.
- (17) Karlsson, S.; Boixel, J.; Pellegrin, Y.; Blart, E.; Becker, H. C.; Odobel, F.; Hammarström, L. Accumulative electron transfer: Multiple charge separation in artificial photosynthesis. *Faraday Discuss.* **2012**, *155*, 233–252.
- (18) Arias-Rotondo, D. M.; McCusker, J. K. The photophysics of photoredox catalysis: a roadmap for catalyst design. *Chem. Soc. Rev.* **2016**, *45*, 5803–5820.
- (19) Housecroft, C. E.; Constable, E. C. The emergence of copper(I)-based dye sensitized solar cells. *Chem. Soc. Rev.* **2015**, *44*, 8386–8398.
- (20) Bharmoria, P.; Bildirir, H.; Moth-Poulsen, K. Triplet-triplet annihilation based near infrared to visible molecular photon upconversion. *Chem. Soc. Rev.* **2020**, *49*, 6529–6554.
- (21) Heinemann, F.; Karges, J.; Gasser, G. Critical overview of the use of Ru(II) polypyridyl complexes as photosensitizers in one-photon and two-photon photodynamic therapy. *Acc. Chem. Res.* **2017**, *50*, 2727–2736.
- (22) Förster, C.; Heinze, K. Photophysics and photochemistry with earth-abundant metals – fundamentals and concepts. *Chem. Soc. Rev.* **2020**, *49*, 1057–1070.
- (23) Wenger, O. S. Photoactive Complexes with Earth-Abundant Metals. *J. Am. Chem. Soc.* **2018**, *140*, 13522–13533.
- (24) Hockin, B. M.; Li, C. F.; Robertson, N.; Zysman-Colman, E. Photoredox Catalysts Based on Earth-Abundant Metal Complexes. *Catal. Sci. Technol.* **2019**, *9*, 889–915.
- (25) Dietrich-Buchecker, C. O.; Marnot, P. A.; Sauvage, J. P.; Kirchoff, J. R.; McMillin, D. R. Bis(2,9-Diphenyl-1,10-phenanthroline)copper(I) - A Copper Complex With a Long-Lived Charge Transfer Excited State. *J. Chem. Soc., Chem. Commun.* **1983**, 513–515.
- (26) Maestri, M.; Bolletta, F.; Moggi, L.; Balzani, V.; Henry, M. S.; Hoffman, M. Z. Mechanism of Photochemistry and Photophysics of Tris(2,2'-Bipyridine)chromium(III) ion in Aqueous Solution. *J. Am. Chem. Soc.* **1978**, *100*, 2694–2701.
- (27) Heinze, K.; Förster, C.; Vöhringer, P.; Sarkar, B. Licht und Leuchten bei 3d-Metallen. *Nachr. Chem.* **2019**, *67*, 54–59.
- (28) Viaene, L.; D'Olieslager, J. Luminescence from and absorption by the <sup>3</sup>T<sub>1g</sub> Level of the Hexacyanocobaltate(III) Ion. *Inorg. Chem.* **1987**, *26*, 960–962.
- (29) Chábera, P.; Liu, Y.; Prakash, O.; Thyraug, E.; El Nahhas, A.; Honarfar, A.; Essén, S.; Fredin, L. A.; Harlang, T. C. B.; Kjaer, K. S.; Handrup, K.; Ericsson, F.; Tatsuno, Y.; Morgan, K.; Schnadt, J.; Häggström, L.; Ericsson, T.; Sobkowiak, A.; Lidin, S.; Huang, P.; Styring, S.; Uhlig, J.; Bendix, J.; Lomoth, R.; Sundström, V.; Persson, P.; Wärnmark, K. A low-spin Fe<sup>III</sup> complex with 100-ps ligand-to-metal charge transfer photoluminescence. *Nature* **2017**, *543*, 695–699.
- (30) Kjær, K. S.; Kaul, N.; Prakash, O.; Chábera, P.; Rosemann, N. W.; Honarfar, A.; Gordivska, O.; Fredin, L. A.; Bergquist, K. E.; Haggstrom, L.; Ericsson, T.; Lindh, L.; Yartsev, A.; Styring, S.; Huang, P.; Uhlig, J.; Bendix, J.; Strand, D.; Sundström, V.; Persson, P.; Lomoth, R.; Wärnmark, K. Luminescence and reactivity of a charge-transfer excited iron complex with nanosecond lifetime. *Science* **2019**, *363*, 249–253.
- (31) Young, E. R.; Oldacre, A. Iron Hits the Mark. *Science* **2019**, *363*, 225–226.
- (32) Herr, P.; Kerzig, C.; Larsen, C. B.; Häussinger, D.; Wenger, O. S. Manganese(I) complexes with metal-to-ligand charge transfer luminescence and photoreactivity. *Nat. Chem.* **2021**, DOI: 10.1038/s41557-021-00744-9.
- (33) Dorn, M.; Kalmbach, J.; Boden, P.; Kruse, A.; Dab, C.; Reber, C.; Niedner-Schatteburg, G.; Lochbrunner, S.; Gerhards, M.; Seitz, M.; Heinze, K. Ultrafast and long-time excited state kinetics of an NIR-emissive vanadium(III) complex I: Synthesis, spectroscopy and static quantum chemistry. *Chem. Sci.* **2021**, *12*, 10780–10790.
- (34) Dorn, M.; Kalmbach, J.; Boden, P.; Pápcke, A.; Gómez, S.; Förster, C.; Kuczelinis, F.; Carrella, L. M.; Büldt, L. A.; Bings, N. H.; Rentschler, E.; Lochbrunner, S.; González, L.; Gerhards, M.; Seitz, M.; Heinze, K. A Vanadium(III) Complex with Blue and NIR-II Spin-Flip Luminescence in Solution. *J. Am. Chem. Soc.* **2020**, *142*, 7947–7955.
- (35) Tungulin, D.; Leier, J.; Carter, A. B.; Powell, A. K.; Albuquerque, R. Q.; Unterreiner, A. N.; Bizzarri, C. Chasing BODIPY: Enhancement of Luminescence in Homoleptic Bis(dipyrrinato) Zn<sup>II</sup> Complexes Utilizing Symmetric and Unsymmetrical Dipyrrins. *Chem. - Eur. J.* **2019**, *25*, 3816–3827.
- (36) Lazorski, M. S.; Castellano, F. N. Advances in the Light Conversion Properties of Cu(I)-Based Photosensitizers. *Polyhedron* **2014**, *82*, 57–70.
- (37) Gernert, M.; Müller, U.; Haehnel, M.; Pflaum, J.; Steffen, A. A Cyclic Alkyl(amino)carbene as Two-Atom  $\pi$ -Chromophore Leading to the First Phosphorescent Linear Cu<sup>I</sup> Complexes. *Chem. - Eur. J.* **2017**, *23*, 2206–2216.
- (38) Hamze, R.; Peltier, J. L.; Sylvinson, D.; Jung, M.; Cardenas, J.; Haiges, R.; Soleilhavoup, M.; Jazzar, R.; Djurovich, P. I.; Bertrand, G.; Thompson, M. E. Eliminating nonradiative decay in Cu<sup>I</sup> emitters: > 99% quantum efficiency and microsecond lifetime. *Science* **2019**, *363*, 601–606.
- (39) Shi, S.; Jung, M. C.; Coburn, C.; Tadle, A.; Sylvinson, M. R. D.; Djurovich, P. I.; Forrest, S. R.; Thompson, M. E. Highly Efficient Photo- and Electroluminescence from Two-Coordinate Cu(I) Complexes Featuring Nonconventional N-Heterocyclic Carbenes. *J. Am. Chem. Soc.* **2019**, *141*, 3576–3588.
- (40) Chen, L. X.; Shaw, G. B.; Novozhilova, I.; Liu, T.; Jennings, G.; Attenkofer, K.; Meyer, G. J.; Coppens, P. MLCT state structure and dynamics of a copper(I) diimine complex characterized by pump-

probe X-ray and laser spectroscopies and DFT calculations. *J. Am. Chem. Soc.* **2003**, *125*, 7022–7034.

(41) Li, T.-y.; Muthiah Ravinson, D. S.; Haiges, R.; Djurovich, P. I.; Thompson, M. E. Enhancement of the Luminescent Efficiency in Carbene-Au(I)-Aryl Complexes by the Restriction of Renner–Teller Distortion and Bond Rotation. *J. Am. Chem. Soc.* **2020**, *142*, 6158–6172.

(42) Di, D. W.; Romanov, A. S.; Yang, L.; Richter, J. M.; Rivett, J. P. H.; Jones, S.; Thomas, T. H.; Jalebi, M. A.; Friend, R. H.; Linnolahti, M.; Bochmann, M.; Credginton, D. High-performance light-emitting diodes based on carbene-metal-amides. *Science* **2017**, *356*, 159–163.

(43) Shaw, G. B.; Grant, C. D.; Shirota, H.; Castner, E. W.; Meyer, G. J.; Chen, L. X. Ultrafast Structural Rearrangements in the MLCT Excited State for Copper(I) bis-Phenanthrolines in Solution. *J. Am. Chem. Soc.* **2007**, *129*, 2147–2160.

(44) Chen, L. X.; Jennings, G.; Liu, T.; Gosztola, D. J.; Hessler, J. P.; Scaltrito, D. V.; Meyer, G. J. Rapid excited-state structural reorganization captured by pulsed X-rays. *J. Am. Chem. Soc.* **2002**, *124*, 10861–10867.

(45) Gernert, M.; Balles-Wolf, L.; Kerner, F.; Müller, U.; Schmiedel, A.; Holzapfel, M.; Marian, C. M.; Pflaum, J.; Lambert, C.; Steffen, A. Cyclic (Amino)arylcarbenes Enter the Field of Chromophore Ligands: Expanded  $\pi$  System Leads to Unusually Deep Red Emitting Cu<sup>I</sup> Compounds. *J. Am. Chem. Soc.* **2020**, *142*, 8897–8909.

(46) Büldt, L. A.; Guo, X.; Vogel, R.; Prescimone, A.; Wenger, O. S. A tris(diisocyanide)chromium(0) complex is a luminescent analog of Fe(2,2'-bipyridine)<sub>3</sub><sup>2+</sup>. *J. Am. Chem. Soc.* **2017**, *139*, 985–992.

(47) Wegeberg, C.; Häussinger, D.; Wenger, O. S. Pyrene-Decoration of a Chromium(0) Tris(Diisocyanide) Enhances Excited State Delocalization: A Strategy to Improve the Photoluminescence of 3d<sup>6</sup> Metal Complexes. *J. Am. Chem. Soc.* **2021**, DOI: 10.1021/jacs.1c07345.

(48) Cope, J. D.; Denny, J. A.; Lamb, R. W.; McNamara, L. E.; Hammer, N. I.; Webster, C. E.; Hollis, T. K. Synthesis, characterization, photophysics, and a ligand rearrangement of CCC-NHC pincer nickel complexes: Colors, polymorphs, emission, and Raman spectra. *J. Organomet. Chem.* **2017**, *845*, 258–265.

(49) Wong, Y. S.; Tang, M. C.; Ng, M. G.; Yam, V. W. W. Toward the Design of Phosphorescent Emitters of Cyclometalated Earth-Abundant Nickel(II) and Their Supramolecular Study. *J. Am. Chem. Soc.* **2020**, *142*, 7638–7646.

(50) Pfennig, B. W.; Thompson, M. E.; Bocarsly, A. B. A new class of room temperature luminescent organometallic complexes: luminescence and photophysical properties of permethylscandocene chloride in fluid solution. *J. Am. Chem. Soc.* **1989**, *111*, 8947–8948.

(51) Bauer, M.; Steube, J.; Pöpcke, A.; Bokareva, O.; Reuter, T.; Demeshko, S.; Schoch, R.; Hohloch, S.; Meyer, F.; Heinze, K.; Kühn, O.; Lochbrunner, S., Janus-type dual emission of a Cyclometalated Iron(III) complex. *Research Square*, September 4, **2020**, ver. 1. DOI: 10.21203/rs.3.rs-64316/v1.

(52) Pal, A. K.; Li, C. F.; Hanan, G. S.; Zysman-Colman, E. Blue-emissive cobalt(III) complexes and their use in the photocatalytic trifluoromethylation of polycyclic aromatic hydrocarbons. *Angew. Chem., Int. Ed.* **2018**, *57*, 8027–8031.

(53) Cuttall, D. G.; Kuang, S. M.; Fanwick, P. E.; McMillin, D. R.; Walton, R. A. Simple Cu(I) Complexes with Unprecedented Excited-State Lifetimes. *J. Am. Chem. Soc.* **2002**, *124*, 6–7.

(54) Ford, P. C.; Cariati, E.; Bourassa, J. Photoluminescence properties of multinuclear copper(I) compounds. *Chem. Rev.* **1999**, *99*, 3625–3647.

(55) Dias, H. V. R.; Diyalanage, H. V. K.; Eldabaja, M. G.; Elbjairami, O.; Rawashdeh-Omary, M. A.; Omary, M. A. Brightly Phosphorescent Trinuclear Copper(I) Complexes of Pyrazolates: Substituent Effects on the Supramolecular Structure and Photophysics. *J. Am. Chem. Soc.* **2005**, *127*, 7489–7501.

(56) Yam, V. W. W.; Lo, K. K. W. Luminescent polynuclear d<sup>10</sup> metal complexes. *Chem. Soc. Rev.* **1999**, *28*, 323–334.

(57) Hossain, A.; Bhattacharyya, A.; Reiser, O. Copper's rapid ascent in visible-light photoredox catalysis. *Science* **2019**, *364*, eaav9713.

(58) Heberle, M.; Tschierlei, S.; Rockstroh, N.; Ringenberg, M.; Frey, W.; Junge, H.; Beller, M.; Lochbrunner, S.; Karnahl, M. Heteroleptic Copper Photosensitizers: Why an Extended  $\pi$ -System Does Not Automatically Lead to Enhanced Hydrogen Production. *Chem. - Eur. J.* **2017**, *23*, 312–319.

(59) Larsen, C. B.; Wenger, O. S. Photoredox Catalysis with Metal Complexes Made from Earth-Abundant Elements. *Chem. - Eur. J.* **2018**, *24*, 2039–2058.

(60) Hernandez-Perez, A. C.; Collins, S. K. Heteroleptic Cu-Based Sensitizers in Photoredox Catalysis. *Acc. Chem. Res.* **2016**, *49*, 1557–1565.

(61) Rentschler, M.; Schmid, M. A.; Frey, W.; Tschierlei, S.; Karnahl, M. Multidentate Phenanthroline Ligands Containing Additional Donor Moieties and Their Resulting Cu(I) and Ru(II) Photosensitizers: A Comparative Study. *Inorg. Chem.* **2020**, *59*, 14762–14771.

(62) Rosko, M. C.; Wells, K. A.; Hauke, C. E.; Castellano, F. N. Next Generation Cuprous Phenanthroline MLCT Photosensitizer Featuring Cyclohexyl Substituents. *Inorg. Chem.* **2021**, *60*, 8394–8403.

(63) Yam, V. W. W.; Wong, K. M. C. Luminescent metal complexes of d<sup>6</sup>, d<sup>8</sup> and d<sup>10</sup> transition metal centres. *Chem. Commun.* **2011**, *47*, 11579–11592.

(64) Juris, A.; Balzani, V.; Barigelletti, F.; Campagna, S.; Belser, P.; Von Zelewsky, A. Ru(II) Polypyridine Complexes - Photophysics, Photochemistry, Electrochemistry, and Chemi-Luminescence. *Coord. Chem. Rev.* **1988**, *84*, 85–277.

(65) Wenger, O. S. Is Iron the New Ruthenium? *Chem. - Eur. J.* **2019**, *25*, 6043–6052.

(66) Zhang, W. K.; Gaffney, K. J. Mechanistic Studies of Photoinduced Spin Crossover and Electron Transfer in Inorganic Complexes. *Acc. Chem. Res.* **2015**, *48*, 1140–1148.

(67) Auböck, G.; Chergui, M. Sub-50-fs photoinduced spin crossover in Fe(bpy)<sub>3</sub><sup>2+</sup>. *Nat. Chem.* **2015**, *7*, 629–633.

(68) Woodhouse, M. D.; McCusker, J. K. Mechanistic Origin of Photoredox Catalysis Involving Iron(II) Polypyridyl Chromophores. *J. Am. Chem. Soc.* **2020**, *142*, 16229–16233.

(69) Gualandi, A.; Marchini, M.; Mengozzi, L.; Natali, M.; Lucarini, M.; Ceroni, P.; Cozzi, P. G. Organocatalytic Enantioselective Alkylation of Aldehydes with [Fe(bpy)<sub>3</sub>]Br<sub>2</sub> Catalyst and Visible Light. *ACS Catal.* **2015**, *5*, 5927–5931.

(70) Parisien-Collette, S.; Hernandez-Perez, A. C.; Collins, S. K. Photochemical Synthesis of Carbazoles Using an [Fe(phen)<sub>3</sub>](NTf<sub>2</sub>)<sub>2</sub>/O<sub>2</sub> Catalyst System: Catalysis toward Sustainability. *Org. Lett.* **2016**, *18*, 4994–4997.

(71) Zhou, W.-J.; Wu, X.-D.; Miao, M.; Wang, Z.-H.; Chen, L.; Shan, S.-Y.; Cao, G.-M.; Yu, D.-G. Light Runs Across Iron Catalysts in Organic Transformations. *Chem. - Eur. J.* **2020**, *26*, 15052–15064.

(72) Tatsuno, H.; Kjær, K. S.; Kunus, K.; Harlang, T. C. B.; Timm, C.; Guo, M.; Chàbera, P.; Fredin, L. A.; Hartsock, R. W.; Reinhard, M. E.; Koroidov, S.; Li, L.; Cordones, A. A.; Gordivska, O.; Prakash, O.; Liu, Y.; Laursen, M. G.; Biasin, E.; Hansen, F. B.; Vester, P.; Christensen, M.; Haldrup, K.; Németh, Z.; Sárosiné Szemes, D.; Bajnóczi, É.; Vankó, G.; Van Driel, T. B.; Alonso-Mori, R.; Glowina, J. M.; Nelson, S.; Sikorski, M.; Lemke, H. T.; Sokaras, D.; Canton, S. E.; Dohn, A. O.; Möller, K. B.; Nielsen, M. M.; Gaffney, K. J.; Wärnmark, K.; Sundström, V.; Persson, P.; Uhlig, J. Hot Branching Dynamics in a Light-Harvesting Iron Carbene Complex Revealed by Ultrafast X-ray Emission Spectroscopy. *Angew. Chem., Int. Ed.* **2020**, *59*, 364–372.

(73) Braun, J. D.; Lozada, I. B.; Kolodziej, C.; Burda, C.; Newman, K. M. E.; van Lierop, J.; Davis, R. L.; Herbert, D. E. Iron(II) coordination complexes with panchromatic absorption and nanosecond charge-transfer excited state lifetimes. *Nat. Chem.* **2019**, *11*, 1144–1150.

(74) Paulus, B. C.; Adelman, S. L.; Jamula, L. L.; McCusker, J. K. Leveraging excited-state coherence for synthetic control of ultrafast dynamics. *Nature* **2020**, *582*, 214–218.

(75) Vittardi, S. B.; Magar, R. T.; Schrage, B. R.; Ziegler, C. J.; Jakubikova, E.; Rack, J. J. Evidence for a lowest energy <sup>3</sup>MLCT

- excited state in  $[\text{Fe}(\text{tpy})(\text{CN})_3]^-$ . *Chem. Commun.* **2021**, *57*, 4658–4661.
- (76) Reuter, T.; Kruse, A.; Schoch, R.; Lochbrunner, S.; Bauer, M.; Heinze, K. Higher MLCT lifetime of carbene iron(II) complexes by chelate ring expansion. *Chem. Commun.* **2021**, *57*, 7541–7544.
- (77) Liu, Y. Z.; Persson, P.; Sundström, V.; Wärnmark, K. Fe N-heterocyclic carbene complexes as promising photosensitizers. *Acc. Chem. Res.* **2016**, *49*, 1477–1485.
- (78) Duchanois, T.; Liu, L.; Pastore, M.; Monari, A.; Cebrian, C.; Trolez, Y.; Darari, M.; Magra, K.; Frances-Monerris, A.; Domenichini, E.; Beley, M.; Assfeld, X.; Haacke, S.; Gros, P. C. NHC-based iron sensitizers for DSSCs. *Inorganics* **2018**, *6*, 63.
- (79) Ashley, D. C.; Jakubikova, E. Ironing out the Photochemical and Spin-Crossover Behavior of Fe(II) Coordination Compounds with Computational Chemistry. *Coord. Chem. Rev.* **2017**, *337*, 97–111.
- (80) Kurz, H.; Schötz, K.; Papadopoulos, I.; Heinemann, F. W.; Maid, H.; Guldi, D. M.; Köhler, A.; Hörner, G.; Weber, B. A Fluorescence-Detected Coordination-Induced Spin State Switch. *J. Am. Chem. Soc.* **2021**, *143*, 3466–3480.
- (81) Mann, K. R.; Gray, H. B.; Hammond, G. S. Excited-state reactivity patterns of hexakisarylisocyanide complexes of chromium(0), molybdenum(0), and tungsten(0). *J. Am. Chem. Soc.* **1977**, *99*, 306–307.
- (82) Sattler, W.; Henling, L. M.; Winkler, J. R.; Gray, H. B. Bespoke photoreductants: tungsten aryisocyanides. *J. Am. Chem. Soc.* **2015**, *137*, 1198–1205.
- (83) Büldt, L. A.; Guo, X.; Prescimone, A.; Wenger, O. S. A Molybdenum(0) Isocyanide Analogue of  $\text{Ru}(2,2'\text{-Bipyridine})_3^{2+}$ : A Strong Reductant for Photoredox Catalysis. *Angew. Chem., Int. Ed.* **2016**, *55*, 11247–11250.
- (84) Herr, P.; Glaser, F.; Büldt, L. A.; Larsen, C. B.; Wenger, O. S. Long-lived, strongly emissive, and highly reducing excited states in Mo(0) complexes with chelating isocyanides. *J. Am. Chem. Soc.* **2019**, *141*, 14394–14402.
- (85) Bilger, J. B.; Kerzig, C.; Larsen, C. B.; Wenger, O. S. A Photorobust Mo(0) Complex Mimicking  $[\text{Os}(2,2'\text{-bipyridine})_3]^{2+}$  and Its Application in Red-to-Blue Upconversion. *J. Am. Chem. Soc.* **2021**, *143*, 1651–1663.
- (86) McCusker, C. E.; Castellano, F. N. Design of a Long-Lifetime, Earth-Abundant, Aqueous Compatible Cu(I) Photosensitizer Using Cooperative Steric Effects. *Inorg. Chem.* **2013**, *52*, 8114–8120.
- (87) Zhang, Y.; Lee, T. S.; Favale, J. M.; Leary, D. C.; Petersen, J. L.; Scholes, G. D.; Castellano, F. N.; Milsmann, C. Delayed fluorescence from a zirconium(IV) photosensitizer with ligand-to-metal charge-transfer excited states. *Nat. Chem.* **2020**, *12*, 345–352.
- (88) Manuta, D. M.; Lees, A. J. Emission and photochemistry of  $\text{M}(\text{CO})_4(\text{diimine})$  (M = chromium, molybdenum, tungsten) complexes in room-temperature solution. *Inorg. Chem.* **1986**, *25*, 1354–1359.
- (89) Lees, A. J. Luminescence properties of organometallic complexes. *Chem. Rev.* **1987**, *87*, 711–743.
- (90) Röhrs, M.; Escudero, D. Multiple Anti-Kasha Emissions in Transition-Metal Complexes. *J. Phys. Chem. Lett.* **2019**, *10*, 5798–5804.
- (91) Farrell, I. R.; Matousek, P.; Towrie, M.; Parker, A. W.; Grills, D. C.; George, M. W.; Vlček, A. Direct Observation of Competitive Ultrafast CO Dissociation and Relaxation of an MLCT Excited State: Picosecond Time-Resolved Infrared Spectroscopic Study of  $[\text{Cr}(\text{CO})_4(2,2'\text{-bipyridine})]$ . *Inorg. Chem.* **2002**, *41*, 4318–4323.
- (92) Howarth, A. J.; Majewski, M. B.; Wolf, M. O. Photophysical properties and applications of coordination complexes incorporating pyrene. *Coord. Chem. Rev.* **2015**, *282*, 139–149.
- (93) McClenaghan, N. D.; Barigelletti, F.; Maubert, B.; Campagna, S. Towards ruthenium(II) polypyridine complexes with prolonged and predetermined excited state lifetimes. *Chem. Commun.* **2002**, 602–603.
- (94) Dierks, P.; Papcke, A.; Bokareva, O. S.; Altenburger, B.; Reuter, T.; Heinze, K.; Kuhn, O.; Lochbrunner, S.; Bauer, M. Ground- and Excited-State Properties of Iron(II) Complexes Linked to Organic Chromophores. *Inorg. Chem.* **2020**, *59*, 14746–14761.
- (95) Boden, P.; Di Martino-Fumo, P.; Bens, T.; Steiger, S.; Albold, U.; Niedner-Schatteburg, G.; Gerhards, M.; Sarkar, B. NIR-Emissive Chromium(0), Molybdenum(0), and Tungsten(0) Complexes in the Solid State at Room Temperature. *Chem. - Eur. J.* **2021**, *27*, 12959.
- (96) Henke, W. C.; Otolski, C. J.; Moore, W. N. G.; Elles, C. G.; Blakemore, J. D. Ultrafast Spectroscopy of  $[\text{Mn}(\text{CO})_3]$  Complexes: Tuning the Kinetics of Light-Driven CO Release and Solvent Binding. *Inorg. Chem.* **2020**, *59*, 2178–2187.
- (97) Kottelat, E.; Lucarini, F.; Crochet, A.; Ruggi, A.; Zobi, F. Correlation of MLCTs of Group 7  $\text{fac-M}(\text{CO})_3^+$  Complexes (M = Mn, Re) with Bipyridine, Pyridinylpyrazine, Azopyridine, and Pyridin-2-ylmethanimine Type Ligands for Rational photoCORM Design. *Eur. J. Inorg. Chem.* **2019**, *2019*, 3758–3768.
- (98) Schatzschneider, U. PhotoCORMs: Light-triggered release of carbon monoxide from the coordination sphere of transition metal complexes for biological applications. *Inorg. Chim. Acta* **2011**, *374*, 19–23.
- (99) Holleman, A. F.; Wiberg, N. *Lehrbuch der Anorganischen Chemie*, 102nd ed.; Walter de Gruyter: Berlin, 2007.
- (100) Ting, S. I.; Garakyaraghi, S.; Taliaferro, C. M.; Shields, B. J.; Scholes, G. D.; Castellano, F. N.; Doyle, A. G.  $^3\text{d-d}$  Excited States of Ni(II) Complexes Relevant to Photoredox Catalysis: Spectroscopic Identification and Mechanistic Implications. *J. Am. Chem. Soc.* **2020**, *142*, 5800–5810.
- (101) Tian, L.; Till, N. A.; Kudisch, B.; MacMillan, D. W. C.; Scholes, G. D. Transient Absorption Spectroscopy Offers Mechanistic Insights for an Iridium/Nickel-Catalyzed C-O Coupling. *J. Am. Chem. Soc.* **2020**, *142*, 4555–4559.
- (102) Welin, E. R.; Le, C.; Arias-Rotondo, D. M.; McCusker, J. K.; MacMillan, D. W. C. Photosensitized, Energy Transfer-Mediated Organometallic Catalysis through Electronically Excited Nickel(II). *Science* **2017**, *355*, 380–384.
- (103) Tellis, J. C.; Primer, D. N.; Molander, G. A. Single-electron transmetalation in organoboron cross-coupling by photoredox/nickel dual catalysis. *Science* **2014**, *345*, 433–436.
- (104) Qin, Y. Z.; Sun, R.; Gianoulis, N. P.; Nocera, D. G. Photoredox Nickel-Catalyzed C-S Cross-Coupling: Mechanism, Kinetics, and Generalization. *J. Am. Chem. Soc.* **2021**, *143*, 2005–2015.
- (105) Wenger, O. S. Photoactive Nickel Complexes in Cross-Coupling Catalysis. *Chem. - Eur. J.* **2021**, *27*, 2270–2278.
- (106) Büldt, L. A.; Larsen, C. B.; Wenger, O. S. Luminescent  $\text{Ni}^0$  Diisocyanide Chelates as Analogues of  $\text{Cu}^{\text{I}}$  Diimine Complexes. *Chem. - Eur. J.* **2017**, *23*, 8577–8580.
- (107) Malzkuhn, S.; Wenger, O. S. Luminescent Ni(0) complexes. *Coord. Chem. Rev.* **2018**, *359*, 52–56.
- (108) Grübel, M.; Bosque, I.; Altmann, P. J.; Bach, T.; Hess, C. R. Redox and Photocatalytic Properties of a  $\text{Ni}^{\text{II}}$  Complex with a Macrocyclic Biquinazoline (Mabiq) Ligand. *Chem. Sci.* **2018**, *9*, 3313–3317.
- (109) Lauenstein, R.; Mader, S. L.; Derondeau, H.; Esezobor, O. Z.; Block, M.; Römer, A. J.; Jandl, C.; Riedle, E.; Kaila, V.; Hauer, J.; Thyraug, E.; Hess, C. R. The central role of the metal ion for photoactivity: Zn- vs. Ni-Mabiq. *Chem. Sci.* **2021**, *12*, 7521–7532.
- (110) Pfennig, B. W.; Thompson, M. E.; Bocarsly, A. B. Luminescent  $\text{d}^0$  scandocene complexes: photophysical studies and electronic structure calculations on  $\text{Cp}^*_2\text{ScX}$  (X = Cl, I, Me). *Organometallics* **1993**, *12*, 649–655.
- (111) Kenney, J. W.; Boone, D. R.; Striplin, D. R.; Chen, Y. H.; Hamar, K. B. Electronic luminescence spectra of charge transfer states of titanium(IV) metallocenes. *Organometallics* **1993**, *12*, 3671–3676.
- (112) London, H. C.; Whittemore, T. J.; Gale, A. G.; McMillen, C. D.; Pritchett, D. Y.; Myers, A. R.; Thomas, H. D.; Shields, G. C.; Wagenknecht, P. S. Ligand-to-Metal Charge-Transfer Photophysics and Photochemistry of Emissive  $\text{d}^0$  Titanocenes: A Spectroscopic and Computational Investigation. *Inorg. Chem.* **2021**, *60*, 14399–14409.

- (113) Zhang, Z.; Hilche, T.; Slak, D.; Rietdijk, N. R.; Oloyede, U. N.; Flowers II, R. A.; Gansäuer, A. Titanocenes as Photoredox Catalysts Using Green-Light Irradiation. *Angew. Chem., Int. Ed.* **2020**, *59*, 9355–9359.
- (114) Fermi, A.; Gualandi, A.; Bergamini, G.; Cozzi, P. G. Shining Light on  $Ti^{IV}$  Complexes: Exceptional Tools for Metallaphotoredox Catalysis. *Eur. J. Org. Chem.* **2020**, *2020*, 6955–6965.
- (115) Romain, C.; Choua, S.; Collin, J. P.; Heinrich, M.; Bailly, C.; Karmazin-Brelot, L.; Bellemin-Laponnaz, S.; Dagorne, S. Redox and Luminescent Properties of Robust and Air-Stable N-Heterocyclic Carbene Group 4 Metal Complexes. *Inorg. Chem.* **2014**, *53*, 7371–7376.
- (116) Yang, M.; Sheykhi, S.; Zhang, Y.; Milsman, C.; Castellano, F. N. Low power threshold photochemical upconversion using a zirconium(IV) LMCT photosensitizer. *Chem. Sci.* **2021**, *12*, 9069–9077.
- (117) Zhang, Y.; Lee, T. S.; Petersen, J. L.; Milsman, C. A Zirconium Photosensitizer with a Long-Lived Excited State: Mechanistic Insight into Photoinduced Single-Electron Transfer. *J. Am. Chem. Soc.* **2018**, *140*, S934–S947.
- (118) Zhang, Y.; Petersen, J. L.; Milsman, C. A Luminescent Zirconium(IV) Complex as a Molecular Photosensitizer for Visible Light Photoredox Catalysis. *J. Am. Chem. Soc.* **2016**, *138*, 13115–13118.
- (119) Harris, J. P.; Reber, C.; Colmer, H. E.; Jackson, T. A.; Forshaw, A. P.; Smith, J. M.; Kinney, R. A.; Telser, J. Near-infrared  ${}^2E_g \rightarrow {}^4A_{2g}$  and visible LMCT luminescence from a molecular bis-(tris(carbene)borate) manganese(IV) complex. *Can. J. Chem.* **2017**, *95*, 547–552.
- (120) Duchanois, T.; Etienne, T.; Beley, M.; Assfeld, X.; Perpete, E. A.; Monari, A.; Gros, P. C. Heteroleptic Pyridyl-Carbene Iron Complexes with Tuneable Electronic Properties. *Eur. J. Inorg. Chem.* **2014**, *2014*, 3747–3753.
- (121) Liu, Y. Z.; Harlang, T.; Canton, S. E.; Chábera, P.; Suarez-Alcantara, K.; Fleckhaus, A.; Vithanage, D. A.; Goransson, E.; Corani, A.; Lomoth, R.; Sundström, V.; Wärnmark, K. Towards Longer-Lived Metal-to-Ligand Charge Transfer States of Iron(II) Complexes: An N-Heterocyclic Carbene Approach. *Chem. Commun.* **2013**, *49*, 6412–6414.
- (122) Chábera, P.; Kjaer, K. S.; Prakash, O.; Honarfar, A.; Liu, Y. Z.; Fredin, L. A.; Harlang, T. C. B.; Lidin, S.; Uhlig, J.; Sundström, V.; Lomoth, R.; Persson, P.; Wärnmark, K.  $Fe^{II}$  hexa N-heterocyclic carbene complex with a 528 ps metal-to-ligand charge-transfer excited-state lifetime. *J. Phys. Chem. Lett.* **2018**, *9*, 459–463.
- (123) Mills, I. N.; Porras, J. A.; Bernhard, S. Judicious Design of Cationic, Cyclometalated  $Ir^{III}$  Complexes for Photochemical Energy Conversion and Optoelectronics. *Acc. Chem. Res.* **2018**, *51*, 352–364.
- (124) Rosemann, N. W.; Chábera, P.; Prakash, O.; Kaufhold, S.; Wärnmark, K.; Yartsev, A.; Persson, P. Tracing the Full Bimolecular Photocycle of Iron(III)-Carbene Light Harvesters in Electron-Donating Solvents. *J. Am. Chem. Soc.* **2020**, *142*, 8565–8569.
- (125) Neumann, S.; Wenger, O. S.; Kerzig, C. Controlling Spin-Correlated Radical Pairs with Donor-Acceptor Dyads: A New Concept to Generate Reduced Metal Complexes for More Efficient Photocatalysis. *Chem. - Eur. J.* **2021**, *27*, 4115–4123.
- (126) Kaul, N.; Lomoth, R. The Carbene Cannibal: Photoinduced Symmetry-Breaking Charge Separation in an  $Fe(III)$  N-Heterocyclic Carbene. *J. Am. Chem. Soc.* **2021**, *143*, 10816–10821.
- (127) Wenger, O. S. A bright future for photosensitizers. *Nat. Chem.* **2020**, *12*, 323–324.
- (128) Carey, M. C.; Adelman, S. L.; McCusker, J. K. Insights into the excited state dynamics of  $Fe(II)$  polypyridyl complexes from variable-temperature ultrafast spectroscopy. *Chem. Sci.* **2019**, *10*, 134–144.
- (129) Medlycott, E. A.; Hanan, G. S. Designing Tridentate Ligands for Ruthenium(II) Complexes with Prolonged Room Temperature Luminescence Lifetimes. *Chem. Soc. Rev.* **2005**, *34*, 133–142.
- (130) Jamula, L. L.; Brown, A. M.; Guo, D.; McCusker, J. K. Synthesis and Characterization of a High-Symmetry Ferrous Polypyridyl Complex: Approaching the  ${}^5T_2/{}^3T_1$  Crossing Point for  $Fe^{II}$ . *Inorg. Chem.* **2014**, *53*, 15–17.
- (131) Otto, S.; Grabolle, M.; Förster, C.; Kreitner, C.; Resch-Genger, U.; Heinze, K.  $Cr(dppd)_2^{3+}$ : A Molecular, Water-Soluble, Highly NIR-Emissive Ruby Analogue. *Angew. Chem., Int. Ed.* **2015**, *54*, 11572–11576.
- (132) Beaulac, R.; Tremblay, J. C.; Bussière, G.; Reber, C. Application of near-infrared luminescence spectroscopy to vanadium(III) complexes. Characterization of their electronic ground state. *Can. J. Anal. Sci. Spectrosc.* **2001**, *46*, 152–161.
- (133) Büldt, L. A.; Wenger, O. S. Chromium Complexes for Luminescence, Solar Cells, Photoredox Catalysis, Upconversion, and Phototriggered NO Release. *Chem. Sci.* **2017**, *8*, 7359–7367.
- (134) Wang, C.; Otto, S.; Dorn, M.; Kreidt, E.; Lebon, J.; Srsan, L.; Di Martino-Fumo, P.; Gerhards, M.; Resch-Genger, U.; Seitz, M.; Heinze, K. Deuterated Molecular Ruby with Record Luminescence Quantum Yield. *Angew. Chem., Int. Ed.* **2018**, *57*, 1112–1116.
- (135) Otto, S.; Scholz, N.; Behnke, T.; Resch-Genger, U.; Heinze, K. Thermo-Chromium: A Contactless Optical Molecular Thermometer. *Chem. - Eur. J.* **2017**, *23*, 12131–12135.
- (136) Otto, S.; Harris, J. P.; Heinze, K.; Reber, C. Molecular ruby under pressure. *Angew. Chem., Int. Ed.* **2018**, *57*, 11069–11073.
- (137) Otto, S.; Nauth, A. M.; Emilov, E.; Scholz, N.; Friedrich, A.; Resch-Genger, U.; Lochbrunner, S.; Opatz, T.; Heinze, K. Photo-Chromium: Sensitizer for Visible Light-Induced Oxidative C-H Bond Functionalization - Electron or Energy Transfer? *ChemPhotoChem* **2017**, *1*, 344–349.
- (138) Otto, S.; Dorn, M.; Förster, C.; Bauer, M.; Seitz, M.; Heinze, K. Understanding and Exploiting Long-Lived Near-Infrared Emission of a Molecular Ruby. *Coord. Chem. Rev.* **2018**, *359*, 102–111.
- (139) Förster, C.; Dorn, M.; Reuter, T.; Otto, S.; Davarci, G.; Reich, T.; Carrella, L.; Rentschler, E.; Heinze, K. Ddpd as Expanded Terpyridine: Dramatic Effects of Symmetry and Electronic Properties in First Row Transition Metal Complexes. *Inorganics* **2018**, *6*, 86.
- (140) Reichenauer, F.; Wang, C.; Förster, C.; Boden, P.; Ugur, N.; Báez-Cruz, R.; Kalmbach, J.; Carrella, L.; Rentschler, E.; Ramanan, C.; Niedner-Schatteburg, G.; Gerhards, M.; Seitz, M.; Resch-Genger, U.; Heinze, K. Strongly Red-Emissive Molecular Ruby  $[Cr(bpmp)_2]^{3+}$  surpasses  $[Ru(bpy)_3]^{2+}$ . *J. Am. Chem. Soc.* **2021**, *143*, 11843–11855.
- (141) Tanabe, Y.; Sugano, S. On the Absorption Spectra of Complex Ions II. *J. Phys. Soc. Jpn.* **1954**, *9*, 766–779.
- (142) Jiménez, J. R.; Poncet, M.; Doistau, B.; Besnard, C.; Piguët, C. Luminescent polypyridyl heteroleptic  $Cr^{III}$  complexes with high quantum yields and long excited state lifetimes. *Dalton Trans.* **2020**, *49*, 13528–13532.
- (143) Abrahamsson, M.; Jäger, M.; Osterman, T.; Eriksson, L.; Persson, P.; Becker, H. C.; Johansson, O.; Hammarström, L. A 3.0 ms Room Temperature Excited State Lifetime of a Bistridentate  $Ru^{II}$ -polypyridine Complex for Rod-Like Molecular Arrays. *J. Am. Chem. Soc.* **2006**, *128*, 12616–12617.
- (144) Jiménez, J. R.; Doistau, B.; Cruz, C. M.; Besnard, C.; Cuerva, J. M.; Campagna, A. G.; Piguët, C. Chiral Molecular Ruby  $[Cr(dqp)_2]^{3+}$  with Long-Lived Circularly Polarized Luminescence. *J. Am. Chem. Soc.* **2019**, *141*, 13244–13252.
- (145) Jiménez, J.-R.; Poncet, M.; Míguez-Lago, S.; Grass, S.; Lacour, J.; Besnard, C.; Cuerva, J. M.; Campaña, A. G.; Piguët, C. Bright Long-Lived Circularly Polarized Luminescence in Chiral Chromium(III) Complexes. *Angew. Chem., Int. Ed.* **2021**, *60*, 10095–10102.
- (146) Conti, C.; Castelli, F.; Forster, L. S. Photophysics of  $Cr(CN)_6^{3-}$  and  $Co(CN)_6^{3-}$  in Poly-Alcohol-Water Solutions at Room-Temperature. *J. Phys. Chem.* **1979**, *83*, 2371–2376.
- (147) Treiling, S.; Wang, C.; Förster, C.; Reichenauer, F.; Kalmbach, J.; Boden, P.; Harris, J.; Carrella, L.; Rentschler, E.; Resch-Genger, U.; Reber, C.; Seitz, M.; Gerhards, M.; Heinze, K. Luminescence and Light-Driven Energy and Electron Transfer from an Exceptionally Long-Lived Excited State of a Non-Innocent Chromium(III) Complex. *Angew. Chem., Int. Ed.* **2019**, *58*, 18075–18085.

- (148) Sinha, N.; Jiménez, J. R.; Pfund, B.; Prescimone, A.; Piguet, C.; Wenger, O. S. A near-infrared-II emissive chromium(III) complex. *Angew. Chem., Int. Ed.* **2021**, DOI: 10.1002/anie.202106398.
- (149) Kaufhold, S.; Rosemann, N. W.; Chábera, P.; Lindh, L.; Losada, I. B.; Uhlig, J.; Pascher, T.; Strand, D.; Wärnmark, K.; Yartsev, A.; Persson, P. Microsecond Photoluminescence and Photoreactivity of a Metal-Centered Excited State in a Hexacarbene-Co(III) Complex. *J. Am. Chem. Soc.* **2021**, *143*, 1307–1312.
- (150) Dee, C.; Zinna, F.; Kitzmann, W. R.; Pescitelli, G.; Heinze, K.; Di Bari, L.; Seitz, M. Strong circularly polarized luminescence of an octahedral chromium(III) complex. *Chem. Commun.* **2019**, *55*, 13078–13081.
- (151) Jäger, M.; Kumar, R. J.; Görls, H.; Bergquist, J.; Johansson, O. Facile Synthesis of Bistridentate Ru<sup>II</sup> Complexes Based on 2,6-Di(quinolin-8-yl)pyridyl Ligands: Sensitizers with Microsecond <sup>3</sup>MLCT Excited State Lifetimes. *Inorg. Chem.* **2009**, *48*, 3228–3238.
- (152) Boden, P.; Di Martino-Fumo, P.; Niedner-Schatteburg, G.; Seidel, W.; Heinze, K.; Gerhards, M. Transient FTIR spectroscopy after one- and two-colour excitation on a highly luminescent chromium(III) complex. *Phys. Chem. Chem. Phys.* **2021**, *23*, 13808–13818.
- (153) Dill, R. D.; Portillo, R. I.; Shepard, S. G.; Shores, M. P.; Rappé, A. K.; Damrauer, N. H. Long-Lived Mixed <sup>2</sup>MLCT/MC States in Antiferromagnetically Coupled d<sup>3</sup> Vanadium(II) Bipyridine and Phenanthroline Complexes. *Inorg. Chem.* **2020**, *59*, 14706–14715.
- (154) Joyce, J. P.; Portillo, R. I.; Nite, C. M.; Nite, J. M.; Nguyen, M. P.; Rappé, A. K.; Shores, M. P. Electronic Structures of Cr(III) and V(II) Polypyridyl Systems: Undertones in an Isoelectronic Analogy. *Inorg. Chem.* **2021**, *60*, 12823.
- (155) Wenger, O. S.; Güdel, H. U. Chemical tuning of the photon upconversion properties in Ti<sup>2+</sup>-doped chloride host lattices. *Inorg. Chem.* **2001**, *40*, 5747–5753.
- (156) Zobel, P.; Knoll, T.; González, L. Ultrafast and long-time excited state kinetics of a NIR-emissive vanadium(III) complex II. Elucidating Triplet-to-Singlet Excited-State Dynamics. *Chem. Sci.* **2021**, *12*, 10791–10801.
- (157) Cannizzo, A.; Blanco-Rodríguez, A. M.; El Nahhas, A.; Šebera, J.; Záliš, S.; Vlček, A.; Chergui, M. Femtosecond fluorescence and intersystem crossing in rhenium(I) carbonyl-bipyridine complexes. *J. Am. Chem. Soc.* **2008**, *130*, 8967–8974.
- (158) Fataftah, M. S.; Bayliss, S. L.; Laorenza, D. W.; Wang, X.; Phelan, B. T.; Wilson, C. B.; Mintun, P. J.; Kovos, B. D.; Wasielewski, M. R.; Han, S.; Sherwin, M. S.; Awschalom, D. D.; Freedman, D. E. Trigonal Bipyramidal V<sup>3+</sup> Complex as an Optically Addressable Molecular Qubit Candidate. *J. Am. Chem. Soc.* **2020**, *142*, 20400–20408.
- (159) Büldt, L. A.; Wenger, O. S. Luminescent Complexes Made from Chelating Isocyanide Ligands and Earth-Abundant Metals. *Dalton Trans.* **2017**, *46*, 15175–15177.
- (160) Büldt, L. A.; Wenger, O. S. Chromium(0), Molybdenum(0), and Tungsten(0) Isocyanide Complexes as Luminophores and Photosensitizers with Long-Lived Excited States. *Angew. Chem., Int. Ed.* **2017**, *56*, 5676–5682.
- (161) Wood, C. J.; Summers, G. H.; Clark, C. A.; Kaeffer, N.; Braeutigam, M.; Carbone, L. R.; D’Amario, L.; Fan, K.; Farré, Y.; Narbey, S.; Oswald, F.; Stevens, L. A.; Parmenter, C. D. J.; Fay, M. W.; La Torre, A.; Snape, C. E.; Dietzek, B.; Dini, D.; Hammarström, L.; Pellegrin, Y.; Odobel, F.; Sun, L.; Artero, V.; Gibson, E. A. A comprehensive comparison of dye-sensitized NiO photocathodes for solar energy conversion. *Phys. Chem. Chem. Phys.* **2016**, *18*, 10727–10738.
- (162) Jiménez, J. R.; Doistau, B.; Besnard, C.; Piguet, C. Versatile Heteroleptic Bis-Terdentate Cr<sup>III</sup> Chromophores Displaying Room Temperature Millisecond Excited State Lifetimes. *Chem. Commun.* **2018**, *54*, 13228–13231.
- (163) Guo, D.; Knight, T. E.; McCusker, J. K. Angular Momentum Conservation in Dipolar Energy Transfer. *Science* **2011**, *334*, 1684–1687.
- (164) Strieth-Kalthoff, F.; Glorius, F. Triplet Energy Transfer Photocatalysis: Unlocking the Next Level. *Chem.* **2020**, *6*, 1888–1903.
- (165) Kasha, M. Characterization of Electronic Transitions in Complex Molecules. *Discuss. Faraday Soc.* **1950**, *9*, 14–19.
- (166) Wenger, O. S.; Güdel, H. U. Influence of crystal field parameters on near-infrared to visible photon upconversion in Ti<sup>2+</sup> and Ni<sup>2+</sup> doped halide lattices. *Struct. Bonding (Berlin, Ger.)* **2004**, *106*, 59–70.
- (167) Schmid, L.; Kerzig, C.; Prescimone, A.; Wenger, O. S. Photostable Ruthenium(II) Isocyanoborato Luminophores and Their Use in Energy Transfer and Photoredox Catalysis. *JACS Au* **2021**, *1*, 819–832.
- (168) Mengel, A. K. C.; Förster, C.; Breivogel, A.; Mack, K.; Ochsmann, J. R.; Laquai, F.; Ksenofontov, V.; Heinze, K. A Heteroleptic Push-Pull Substituted Iron(II) Bis(tridentate) Complex with Low-Energy Charge-Transfer States. *Chem. - Eur. J.* **2015**, *21*, 704–714.
- (169) Fajardo, J.; Schwan, J.; Kramer, W. W.; Takase, M. K.; Winkler, J. R.; Gray, H. B. Third-Generation W(CNAr)<sub>6</sub> Photoreductants (CNAr = Fused-Ring and Alkynyl-Bridged Arylisocyanides). *Inorg. Chem.* **2021**, *60*, 3481–3491.
- (170) Chan, K. T.; Lam, T. L.; Yu, D. H.; Du, L.; Phillips, D. L.; Kwong, C. L.; Tong, G. S. M.; Cheng, G.; Che, C. M. Strongly Luminescent Tungsten Emitters with Emission Quantum Yields of up to 84%: TADF and High-Efficiency Molecular Tungsten OLEDs. *Angew. Chem., Int. Ed.* **2019**, *58*, 14896–14900.
- (171) Qiao, Y. S.; Schelter, E. J. Lanthanide Photocatalysis. *Acc. Chem. Res.* **2018**, *51*, 2926–2936.
- (172) Hu, A.; Guo, J.-J.; Pan, H.; Zuo, Z. Selective functionalization of methane, ethane, and higher alkanes by cerium photocatalysis. *Science* **2018**, *361*, 668–672.
- (173) Bestgen, S.; Schoo, C.; Neumeier, B. L.; Feuerstein, T. J.; Zovko, C.; Köppe, R.; Feldmann, C.; Roesky, H. Intensely Photoluminescent Diamidophosphines of the Alkaline-Earth Metals, Aluminum and Zinc. *Angew. Chem., Int. Ed.* **2018**, *57*, 14265–14269.
- (174) Pinter, P.; Schüßlbauer, C. M.; Watt, F. A.; Dickmann, N.; Herbst-Immer, R.; Morgenstern, B.; Grünwald, A.; Ullrich, T.; Zimmer, M.; Hohloch, S.; Guldi, D. M.; Munz, D. Bright luminescent lithium and magnesium carbene complexes. *Chem. Sci.* **2021**, *12*, 7401–7410.
- (175) Maurer, L. A.; Pearce, O. M.; Maharaj, F. D. R.; Brown, N. L.; Amador, C. K.; Damrauer, N. H.; Marshak, M. P. Open for Bismuth: Main Group Metal-to-Ligand Charge Transfer. *Inorg. Chem.* **2021**, *60*, 10137–10146.
- (176) Cerfontaine, S.; Wehlin, S. A. M.; Elias, B.; Troian-Gautier, L. Photostable Polynuclear Ruthenium(II) Photosensitizers Competent for Dehalogenation Photoredox Catalysis at 590 nm. *J. Am. Chem. Soc.* **2020**, *142*, 5549–5555.
- (177) Vittardi, S. B.; Thapa Magar, R.; Breen, D. J.; Rack, J. J. A Future Perspective on Phototriggered Isomerizations of Transition Metal Sulfoxides and Related Complexes. *J. Am. Chem. Soc.* **2021**, *143*, 526–537.
- (178) Wei, F.; Lai, S.-L.; Zhao, S.; Ng, M.; Chan, M.-Y.; Yam, V. W.-W.; Wong, K. M.-C. Ligand Mediated Luminescence Enhancement in Cyclometalated Rhodium(III) Complexes and Their Applications in Efficient Organic Light-Emitting Devices. *J. Am. Chem. Soc.* **2019**, *141*, 12863–12871.
- (179) Whittemore, T. J.; Xue, C.; Huang, J.; Gallucci, J. C.; Turro, C. Single-chromophore single-molecule photocatalyst for the production of dihydrogen using low-energy light. *Nat. Chem.* **2020**, *12*, 180–185.
- (180) Nicholls, T. P.; Burt, L. K.; Simpson, P. V.; Massi, M.; Bissember, A. C. Tricarbonyl Rhenium(I) Tetrazolato and N-Heterocyclic Carbene Complexes: Versatile Visible-Light-Mediated Photoredox Catalysts. *Dalton Trans.* **2019**, *48*, 12749–12754.
- (181) Scattergood, P. A.; Sinopoli, A.; Elliott, P. I. P. Photophysics and photochemistry of 1,2,3-triazole-based complexes. *Coord. Chem. Rev.* **2017**, *350*, 136–154.



(182) Rodriguez, T. M.; Deegbey, M.; Jakubikova, E.; Dempsey, J. L. The ligand-to-metal charge transfer excited state of  $[\text{Re}(\text{dmpe})_3]^{2+}$ . *Photosynth. Res.* **2021**, DOI: 10.1007/s11120-021-00859-7.

(183) Shon, J. H.; Teets, T. S. Molecular Photosensitizers in Energy Research and Catalysis: Design Principles and Recent Developments. *ACS Energy Lett.* **2019**, *4*, 558–566.

(184) Bevernaegie, R.; Wehlin, S. A. M.; Piechota, E. J.; Abraham, M.; Philouze, C.; Meyer, G. J.; Elias, B.; Troian-Gautier, L. Improved Visible Light Absorption of Potent Iridium(III) Photo-oxidants for Excited-State Electron Transfer Chemistry. *J. Am. Chem. Soc.* **2020**, *142*, 2732–2737.

(185) Shon, J. H.; Kim, D.; Rathnayake, M. D.; Sittel, S.; Weaver, J.; Teets, T. S. Photoredox catalysis on unactivated substrates with strongly reducing iridium photosensitizers. *Chem. Sci.* **2021**, *12*, 4069–4078.

(186) Zhong, J. J.; To, W. P.; Liu, Y. G.; Lu, W.; Che, C. M. Efficient Acceptorless Photo-Dehydrogenation of Alcohols and N-Heterocycles with Binuclear Platinum(II) Diphosphite Complexes. *Chem. Sci.* **2019**, *10*, 4883–4889.

(187) Carrara, S.; Aliprandi, A.; Hogan, C. F.; De Cola, L. Aggregation-Induced Electrochemiluminescence of Platinum(II) Complexes. *J. Am. Chem. Soc.* **2017**, *139*, 14605–14610.

(188) Cebrian, C.; Mauro, M. Recent advances in phosphorescent platinum complexes for organic light-emitting diodes. *Beilstein J. Org. Chem.* **2018**, *14*, 1459–1481.

(189) Zobel, J. P.; González, L. The Quest to Simulate Excited-State Dynamics of Transition Metal Complexes. *JACS Au* **2021**, *1*, 1116–1140.